การกระเจิงแบบรามานและการเปล่งแสงของฟิล์มบาง GaAsN บน GaAs

นางสาวปณัฐดา ปานเพ็ชร

RAMAN SCATTERING AND PHOTOLUMINESCENCE OF
GaAsN THIN FILM ON GaAs

Miss Panatda Panpech

A Thesis Submitted in Partial Fulfillment of the Requirements

for the Degree of Master of Science Program in Physics

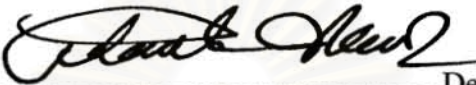Department of Physics

Faculty of Science
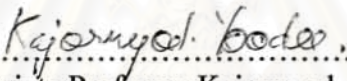
Chulalongkorn University

Academic Year 2006
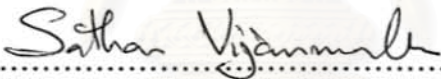
Thesis Title   RAMAN SCATTERING AND PHOTOLUMINESCENCE OF
                      GaAsN THIN FILM ON GaAs
By   Miss Panatda Panpech
Field of study   Physics
Thesis Advisor   Sathon Vijarnwannaluk, Ph.D.
Thesis Co-advisor   Sakuntam Sanorpim, Ph.D.

Accepted by the Faculty of Science, Chulalongkorn University in Partial Fulfillment of the Requirements for the Master's Degree

....Dean of the Faculty of Science
(Professor Piamsak Menasveta, Ph.D.)
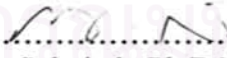
THESIS COMMITTEE

....Chairman
(Associate Professor Kajornyod Yoodee, Ph.D.)

....Thesis Advisor
(Sathon Vijarnwannaluk, Ph.D.)

....Thesis Co-advisor
(Sakuntam Sanorpim, Ph.D.)

....Member
(Somchai Kiatgamolchai, Ph.D.)

....Member
(Jessada Sukpitak, Ph.D.)

iv

ปณัฐดา ปานเพ็ชร : การกระเจิงแบบรามานและการเปล่งแสงของฟิล์มบางแกลเลียมอาร์เซไนด์ ไนไตรด์บนแกลเลียมอาร์เซไนด์. (RAMAN SCATTERING AND PHOTOLUMINESCENCE OF GaAsN THIN FILM ON GaAs) อ. ที่ปรึกษา : อ. ดร. สธน วิจารณ์วรรณลักษณ์, อ.ที่ปรึกษา ร่วม : อ.ดร. สกุลธรรม เสนาะพิมพ์, 56 หน้า.

ฟิล์มบางแกลเลียมอาร์เซไนด์ไนไตรด์ ($GaAs_{1-x}N_x$) ที่ปลูกผลึกลงบนระนาบ (001) ของ แกลเลียมอาร์เซไนด์ (GaAs) ซับสเตรตด้วยวิธีเมทอลออแกนิกเวเปอร์เฟสเอพิแทกซี (Metalorganic Vapor Phase Epitaxy, MOVPE) โดยใช้เธอเชียรีบิวทิลอาร์ซีน (TBAs) และไดเมทธิลไฮดราซีน (DMHy) เป็นสารตั้งต้นของอาร์เซนิก (As) และไนโตรเจน (N) ตามลำดับ ได้ถูกนำมาศึกษาด้วยเทคนิค การกระเจิงแบบรามาน (Raman scattering) ผลการศึกษาสำหรับชุดของฟิล์มบางที่มี N เจือสูงสุดร้อย ละ 5.5 พบโหมดการสั่นของ N แบบโลคอลไลซ์ (Localized Vibrational Mode, LVM) ที่บริเวณ 468 - 475 cm^{-1} จากการศึกษาถึงความสัมพันธ์ระหว่างค่าความเข้มรวมของสัญญาณรามาน (I_{LVM}) และ ค่าความถี่ของโหมดการสั่น LVM ของ N (ω_{LVM}) กับความเข้มข้นของ N พบว่าทั้งสองค่าจะเพิ่มขึ้นเมื่อ ความเข้มข้นของ N มีค่ามากขึ้น และยังพบว่าความเข้มข้นของ N ที่คำนวณด้วยเทคนิคการกระเจิงแบบ รามาน (x_{Raman}) มีความสัมพันธ์แบบเชิงเส้นกับความเข้มข้นของ N ที่คำนวณด้วยเทคนิคการเลี้ยวเบน รังสีเอ็กซ์กำลังแยกสูง (High resolution X-ray Diffraction, HRXRD) (x_{XRD}) ผลจากการวิเคราะห์แสดง ให้เห็นว่าการคำนวณหาความเข้มข้นของ N ด้วยเทคนิคการกระเจิงแบบรามานมีความเหมาะสมและ เชื่อถือได้ เมื่อความเข้มข้นของ N อยู่ในช่วง $x_{XRD} \leq 0.055$

จากผลการทดลองทางแสง แม้ว่าสเปกตรัมที่วัดด้วยเทคนิคฟูเรียร์ทรานสฟอร์มอินฟราเรดส เปกโทรสโกปีของ $GaAs_{1-x}N_x$ จะไม่สามารถสังเกตได้เนื่องจากข้อจำกัดของเครื่องมือวัด แต่ผู้วิจัยได้ทำ การวิเคราะห์ตำแหน่งพลังงานของยอดแหลมการเปล่งแสง (PL peak position) ของ $GaAs_{1-x}N_x$ วัดที่ อุณหภูมิ 8.5 K พบว่าตำแหน่งของยอดแหลมการเปล่งแสงมีการเปลี่ยนแปลงค่าพลังงานตั้งแต่ 1.39 ถึง 0.97 อิเล็กตรอนโวลต์ เมื่อความเข้มข้นของ N มีค่าเพิ่มขึ้นจาก $x_{XRD} = 0.005$ จนถึง 0.0528 ซึ่งการเลื่อน ตำแหน่งของยอดแหลมการเปล่งแสงไปทางพลังงานต่ำอย่างรวดเร็วแสดงให้เห็นว่า $GaAs_{1-x}N_x$ มีค่าโบ วิ่งพารามิเตอร์ (bowing parameter) ที่มีค่ามากเนื่องจากการเติม N เข้าไปในตำแหน่งแลชทิซ (lattice site)

ภาควิชา...ฟิสิกส์.................................... ลายมือชื่อนิสิต.......ปณัฐดา ปานเพ็ชร......
สาขาวิชา...ฟิสิกส์.................................... ลายมือชื่ออาจารย์ที่ปรึกษา....................
ปีการศึกษา...2549.................................... ลายมือชื่ออาจารย์ทีปรึกษาร่วม................

\# \# 477 23577 23   : MAJOR PHYSICS
KEY WORD: GaAsN / HRXRD / RAMAN SCATTERING / LVM / PL

PANATDA   PANPECH   :   RAMAN   SCATTERING   AND PHOTOLUMINESCENCE OF GaAsN THIN FILM ON GaAs.   THESIS ADVISOR : SATHON VIJARNWANNALUK, Ph.D., THESIS COADVISOR : SAKUNTAM SANORPIM, Ph.D., 56 pp.

GaAs$_{1-x}$N$_x$ alloy films ($0 \leq x \leq 0.055$) grown on GaAs (001) substrates by metalorganic vapor phase epitaxy (MOVPE) using TBAs and DMHy as As and N precursors, respectively, were investigated by Raman spectroscopy. It was found that, with incorporating N up to $x = 0.055$, a single N-related localized vibrational mode (LVM) is observed at around 468 - 475 cm^{-1}. We investigated the N-related LVM Raman intensity (I_{LVM}) and frequency (ω_{LVM}) as a function of N concentration. Both the I_{LVM} and the ω_{LVM} were found to rise for the GaAs$_{1-x}$N$_x$ films with higher N incorporation. It is also evident that the N concentration in the GaAs$_{1-x}$N$_x$ grown films determined by Raman spectroscopy technique (x_{Raman}) exhibits a linear dependence on the N concentrations determined by the high resolution X-ray diffraction (HRXRD) (x_{XRD}). Our results demonstrate that the linear dependence of the x_{Raman} on the x_{XRD} provides a useful calibration method to determine the N concentration in dilute GaAs$_{1-x}$N$_x$ films ($x_{XRD} \leq$ 0.055).

Although, the FTIR spectra of GaAs$_{1-x}$N$_x$ films can not be observed due to the limit of the instrument. On the other hand, the 8.5K-PL peak energy of the GaAs$_{1-x}$N$_x$ films was varied from 1.39 to 0.97 eV with increasing N content up to 5.28%. A large red shift in PL peak position demonstrates a large bowing parameter of the GaAs$_{1-x}$N$_x$ alloy layers due to the incorporation of N into the lattice.

Department...Physics......................Student's signature...........................

Field of study...Physics......................Advisor's signature...........................

Academic year...2006......................Co-advisor's signature...........................

ACKNOWLEDGEMENTS

CONTENTS

LIST OF TABLES

LIST OF FIGURES

CHAPTER I

INTRODUCTION

1.1 Motivation

Recently ternary $GaAs_{1-x}N_x$ and quaternary $In_yGa_{1-y}As_{1-x}N_x$ alloys have attracted interests because of their unique electronic and optical characteristics. It is well known that the incorporation of a small amount of N in $GaAs_{1-x}N_x$ leads to a decrease of the bandgap energy due to the large bandgap bowing, and to an increase of the electron effective mass. These alloys have been studied because of their potential applications in long wavelength optoelectronic devices [1, 2] and high efficiency multijunction solar cells [3]. A great deal of work has been done on the epitaxial growth and characterization of the III-V-N type alloys in order to control the bandgap and electrical properties by controlling the alloy composition. While the bandgap and lattice constants as a function of the alloy composition for $GaAs_{1-x}N_x$ have been studied [1 - 4], further work is obviously necessary to investigate the micro-(nano-) structural and optical properties of $GaAs_{1-x}N_x$ as a function of N concentration and to determine the alloying effect of GaN on GaAs.

High resolution X-ray diffraction (HRXRD) is a traditional and powerful technique that has been widely used for crystal structure analysis of epitaxial films [5]. From HRXRD measurement, one can determine the crystalline quality of the $GaAs_{1-x}N_x$ films and the N concentration in the $GaAs_{1-x}N_x$ films.

On the other hand, Raman spectroscopy is a powerful technique to obtain information on crystal structure through measuring the vibrations of the crystal lattice. Raman spectrum provides a sensitive tool for studying the impurity incorporation in the crystal lattice and the structural defects [6]. It is known that for the $GaAs_{1-x}N$ alloy, the N-related localized vibrational mode (LVM) absorption is directly

proportional to the N concentration. Thus, Raman spectroscopy technique can be used to determine the N concentrations in the $GaAs_{1-x}N_x$ epitaxial films.

To investigate the optical properties, low-temperature photoluminescence (LT-PL) is widely used for this alloy system. It is due to the degradation of crystalline quality, which induces an increase in the rate of non-radiative recombination, resulting from the incorporation of N. The LT-PL yields the effects of N incorporation in $GaAs_{1-x}N_x$. In the thesis, structural and optical investigations of $GaAs_{1-x}N_x$ epitaxial films on GaAs are described. The techniques used in this thesis are HRXRD, Raman scattering, Fourier transform infrared spectroscopy, and LT-PL. The goals of this thesis are

1) to determine the N concentration in the $GaAs_{1-x}N_x$ epitaxial films using HRXRD measurements,

2) to apply Raman scattering spectroscopy to determine the N concentration in the $GaAs_{1-x}N_x$ epitaxial films and compare the results with the N concentration determined by HRXRD, and

3) to investigate the relationship between the N concentration and band gap in the $GaAs_{1-x}N_x$ epitaxial films

1.2 Organization of the thesis

The focus of the thesis is to describe the structural and optical properties of $GaAs_{1-x}N_x$, emphasize on the effect of N incorporation. The thesis is organized as follows.

In Chapter II, the knowledge of the characteristic physical properties for the $GaAs_{1-x}N_x$ alloys is presented. The parameters being considered are lattice constant (a), bowing parameter (b), energy gap, etc. The experimental methods (HRXRD, Raman scattering and PL) used in this thesis, and the MOVPE growth information for $GaAs_{1-x}N_x$ samples are presented.

In Chapter III, the structural investigation of $GaAs_{1-x}N_x$ films ($0 \leq x_{XRD} \leq 0.055$) analyzed by HRXRD are described. The N concentration in the $GaAs_{1-x}N_x$ epitaxial films are determined and discussed.

Chapter IV presents the results of Raman scattering study on the $GaAs_{1-x}N_x$ epitaxial films ($0 \leq x_{XRD} \leq 0.055$). Integrated intensity of Raman spectra were used to determine the N concentration in $GaAs_{1-x}N_x$.

Chapter V describes the correlation between PL peak energy and the N concentration of $GaAs_{1-x}N_x$ epitaxial layers. Experimental results are concerned with the effect of N incorporation.

Finally, chapter VI gives the conclusions of this thesis.

CHAPTER II

GaAsN ALLOY AND
EXPERIMENTAL BACKGROUND

2.1 Introduction

The GaAsN alloy semiconductor has attracted considerable attention because of its unique physical properties and its technological application for optoelectronic devices in fiber optic communication networks [4]. The most widely used single-mode optical fiber has a chromatic dispersion minimum at a wavelength of 1.3 μm and an attenuation minimum at 1.55 μm [7]. It also has local attenuation minima at 0.85 μm and 1.3 μm [7]. The properties of the optical fiber have fixed these wavelengths as the optical communications wavelengths [7]. Semiconductor lasers are used as emitters in optical communications. For several years, it has been a lot of research on developing the GaAs-based active material for the optical communication wavelengths. In 1992, a surprise came in the discovery that a significant red shift of the wavelength when a small fraction of N was alloyed into GaAs to form a ternary alloy $GaAs_{1-x}N_x$ [8]. The highly unusual large bandgap reduction achieved by mixing N into GaAs opens the possibility to gain access to the 1.3 and 1.55 μm wavelengths [1, 2, 4, 7, 9]. Due to the very exceptional physical properties of this alloy, the basic parameters such as energy gap (E_g), bowing parameter (b) and lattice constant (a) are necessary to investigate. Thus, this chapter introduces the physical properties of $GaAs_{1-x}N_x$, the preparation of $GaAs_{1-x}N_x$ epitaxial layers, and the experimental methods used in the studies.

2.2 Properties of GaAsN alloy semiconductor

GaAs$_{1-x}$N$_x$ crystallizes in the zincblende (cubic) structure. Figure 2-1 presents the conventional unit cell of GaAs$_{1-x}$N$_x$ where blue, pink and green atoms represent Ga, As and N atoms, respectively. The distinctive properties of the GaAs$_{1-x}$N$_x$ alloy arise from the large size difference between the N and As atoms. Covalent radius of the N atom is 0.068 nm and that of the As atom is 0.121 nm [7]. Physical properties of the GaAs$_{1-x}$N$_x$ alloy have change gradually from the properties of GaAs to that of GaN with increasing N concentration (x). Table 2-1 shows some material parameters of GaAs and cubic phase GaN (c-GaN). Most of the material parameters change linearly on the N concentration (x). The useful method for estimation of the material parameters of any alloy semiconductor is known as the interpolation method [10]. The material parameters (P) of the ternary alloys can be linearly interpolated from the binary data as

$$P_{ABC} = x \cdot P_{AB} + (1-x) \cdot P_{AC} \qquad (2-1)$$

for the AB$_x$C$_{1-x}$ [10]. Some parameters such as lattice constant and elastic stiffness constants, usually have a linear behavior with composition, x, and then Eq. (2-1) gives a good determination for such material parameters. These linear behaviors are known as the Vegard's law. However, for the GaAsN alloy semiconductor, the substantial differences between the properties of the light-atom constituent (GaN) and the heavy-atom constituent (GaAs) contribute the bandgap energy (E_g), usually exhibit nonlinear, and have an approximately quadratic dependence on the composition concentration, x

$$E_{g,GaAsN} = x \cdot E_{g,GaN} + (1-x) \cdot E_{g,GaAs} - b \cdot x \cdot (1-x) \qquad (2-2)$$

where b is the bowing parameter. Most of the researches on the bowing parameter of the GaAs$_{1-x}$N$_x$ alloy semiconductor show that the value of b is huge, and strongly
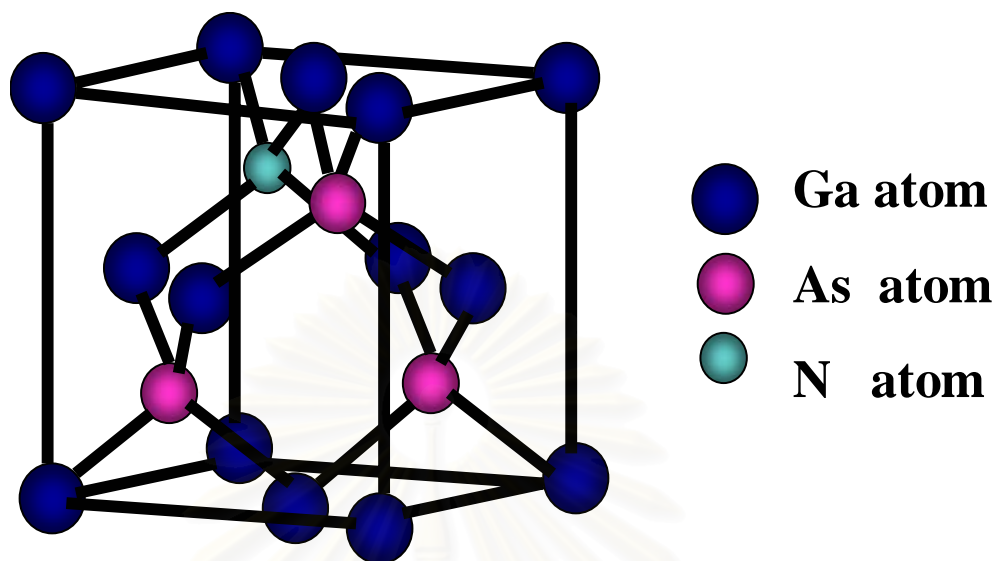
Fig. 2-1 The conventional unit cell of the GaAs$_{1-x}$N$_x$ structure. This structure is the zincblende (cubic) structure. The blue, pink and green atoms represent the Ga, As and N atoms, respectively.

Parameters	GaAs	cubic-GaN
a (Å)	5.653 [7]	4.503 [15]
E_g (eV)	1.424 [16]	3.3 [17]
C_{11} (10^{11} dyn/cm^2)	11.88 [18]	26.4 [15]
C_{12} (10^{11} dyn/cm^2)	5.38 [18]	15.3 [15]

Table 2-1 Some material parameters of GaAs and cubic-GaN obtained at room temperature.
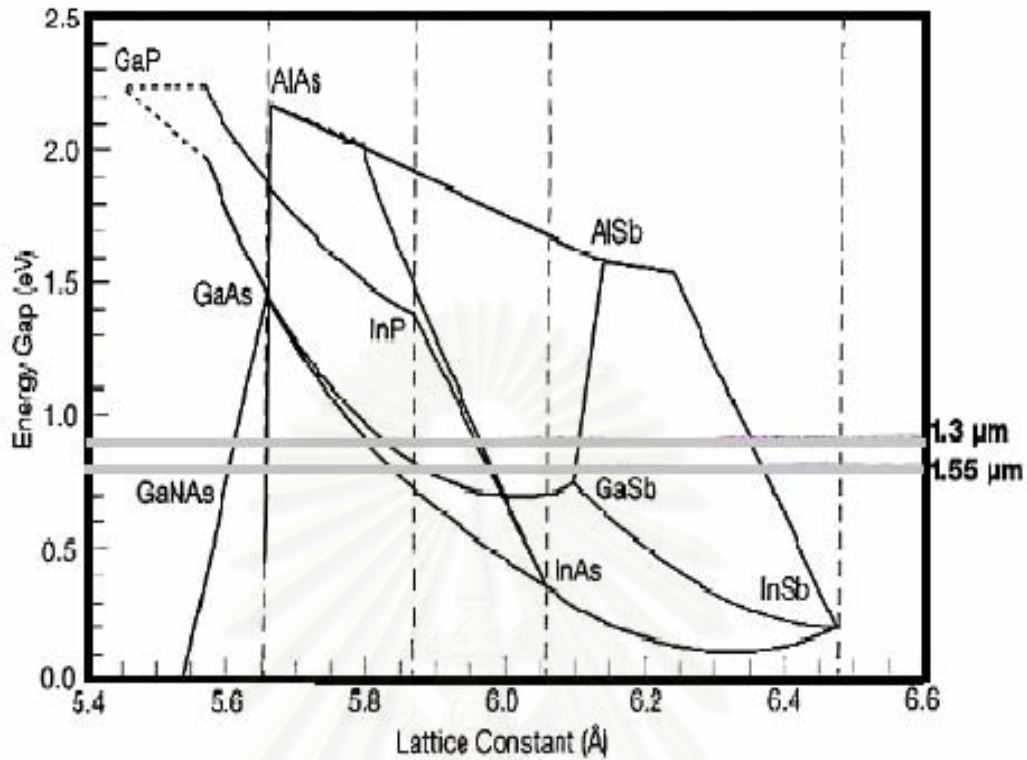
Fig. 2-2 The relationship between lattice constant and energy gap of III-V compound semiconductors. The wavelength 1.3 and 1.55 μm are indicated.

depends on the N concentration (x) [11 - 13]. The recent experimental study on GaAs$_{1-x}$N$_x$ with N fractions as large as 15% confirmed the strong composition dependence of the bowing, with values ranging from 20 eV for dilute alloys to 5 eV for concentrated alloys [14].

Fig. 2-2 presents the relationship between lattice constant (a) and energy gap (E_g) of the III-V compound semiconductors. For example, the isoelectronic substitution of only 1% nitrogen in GaAs reduces the fundamental band gap by ~200 meV, leading to the so-called "giant band gap bowing" [4, 19]. The wavelength at 1.3 and 1.55 μm are indicated, which shows that these wavelength located in the range of the bandgap energy of GaAs$_{1-x}$N$_x$ with a few percents of N concentration.

Consider the elastic vibrations of the crystal; the energy of a lattice vibration is quantized. The quantum of energy of crystal vibration is called the phonon energy [20]. The energy of the phonon is $\hbar\omega$, where the angular frequency is ω. Phonon of wavevector $\vec{k}$ has a momentum $\hbar\vec{k}$. If there are n atom in the primitive cell, the

phonon dispersion relations $\omega(\vec{k})$ will have 3 acoustical phonon branches and $3n$-3 optical phonon branches. Since GaAs has two atoms per unit cell, there are six-phonon branches. These are divided into three optical branches with two transverse and one longitudinal and three acoustic branches with two transverse and one longitudinal. Classification of transverse or longitudinal phonons is according to their displacements which are perpendicular or parallel to the direction of the wave vector. The frequencies of phonon can be determined by several techniques such as the neutrons scattering, infrared reflection, and Raman scattering. Table 2-2 shows the transverse optical (TO) and longitudinal optical (LO) phonon frequencies of GaAs determined from lattice reflection spectra [21]. In Raman scattering process, both energy and wavevector of phonon are conserved [21]. Due to the conservation of wavevector, first-order Raman scattering probes only zone-center phonon ($k = 0$). Observations of the $k = 0$ optical phonon in GaAs are shown in Fig. 2-3 (a). Including in second-order Raman scattering, which is accompanied by the creation of two phonons, or absorption of two phonons, or the creation of one and the absorption of another phonon, the conservation of wavevector is satisfied when $k_a \pm k_b \approx 0$. k_a and k_b are the wavevectors of the phonons a and b, respectively. Second-order Raman spectra have been observed and analyzed in numerous crystals. Measurements on GaAs are shown in Fig. 2-3 (b).

A new vibrational mode that localized around an N atom is appear when the N atom substitutionally replaces an As atom, due to the N atom is lighter than the As atom. This mode is called the localized vibrational mode (LVM) which does not propagate through the crystal. The vibration is around a nitrogen atom and its nearest neighbors [22]. The LVM can be observed by Raman scattering measurement. The LVM at 471 cm^{-1} is used as a quantitative tool to assess the substitutional N fraction [23].

Temperature (K)	ω_T (cm^{-1})	ω_L (cm^{-1})
4.2	273.3	297.3
296	268.2	291.5

Table 2-2 The TO (ω_T) and LO (ω_L) phonon frequencies of GaAs determined from lattice reflection spectra.
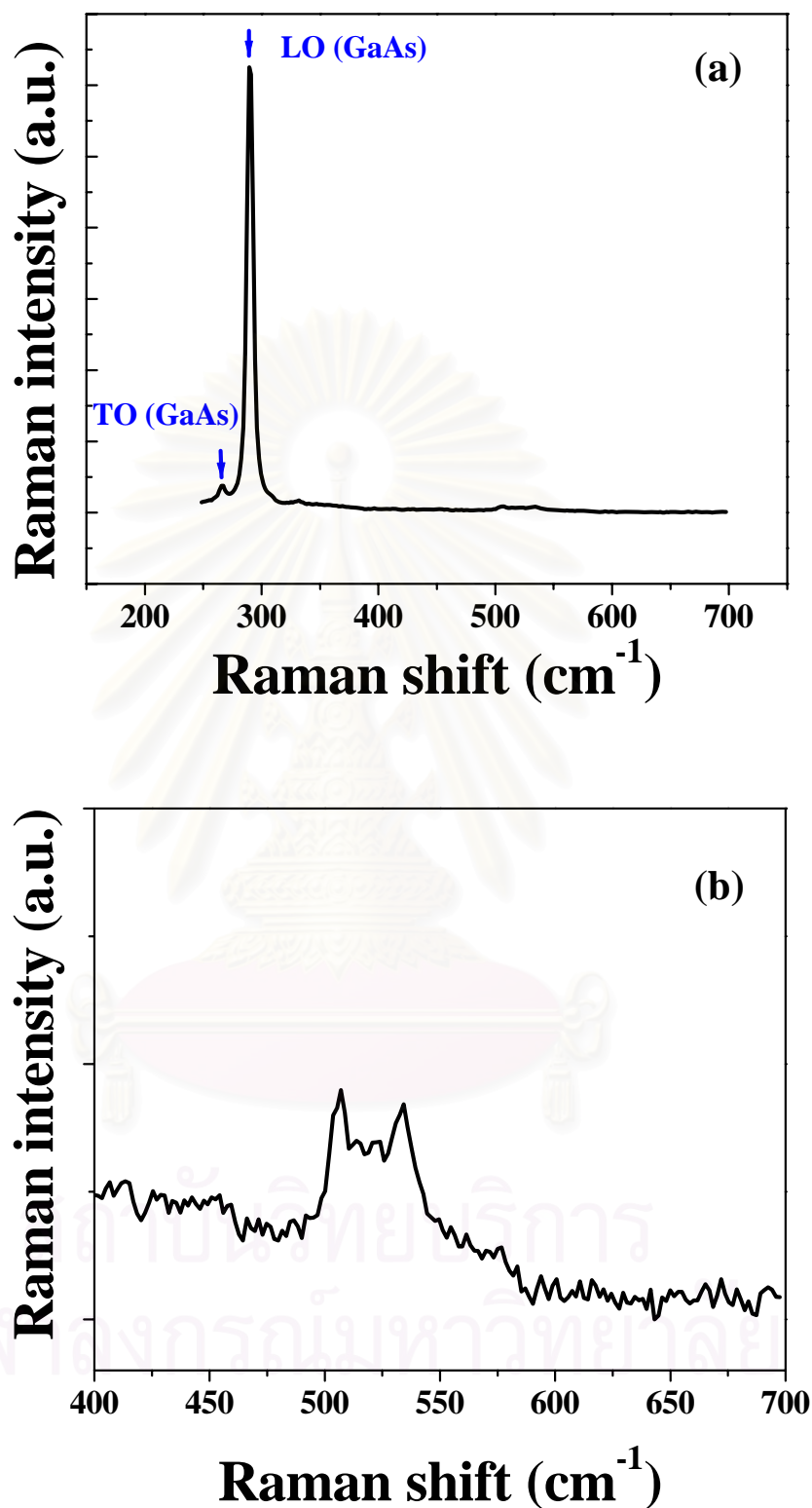
Fig. 2-3 Observation at the $k = 0$ for optical phonon in GaAs is shown in (a). Second-order Raman spectrum on GaAs is shown in (b).

It is known that the integrated intensity of GaAs-LO ($I_{GaAs-LO}$) in GaAs$_{1-x}$N$_x$ is proportional to As concentration and that of N-related LVM (I_{LVM}) is proportional to N concentration. Then x_{Raman} from the Raman measurement can be calculated as follows [4];

$$x_{Raman} = \frac{I_{LVM}}{f \cdot I_{GaAs-LO} + I_{LVM}} \tag{2-3}$$

where f represents the relative N-related LVM oscillator strength with respect to that of the GaAs-LO phonon.

2.3 Experimental background

2.3.1 Preparation of GaAsN alloy samples

GaAs$_{1-x}$N$_x$ epitaxial films used in this study were grown by low-pressure (60 Torr) metalorganic vapor phase epitaxy (MOVPE) at Prof. Kentaro Onabe's Laboratory, Department of Advanced Materials Science, the University of Tokyo [24], Japan. MOVPE growth used trimethylgallium (TMGa), 1, 1-dimethylhydrazine (DMHy), tertiarybutylarsine (TBAs) as the source materials of Ga, N and As, respectively. Ultra-high purity H$_2$ was used as a carrier gas at flow rate of 1.5 slm. All GaAs$_{1-x}$N$_x$ films were nominally un-doped and grown on semi-insulating (SI)

GaAs$_{1-x}$N$_x$	98 – 285 nm
	475 – 550 °C
GaAs buffer	~100 nm
GaAs (001) substrate	700 °C
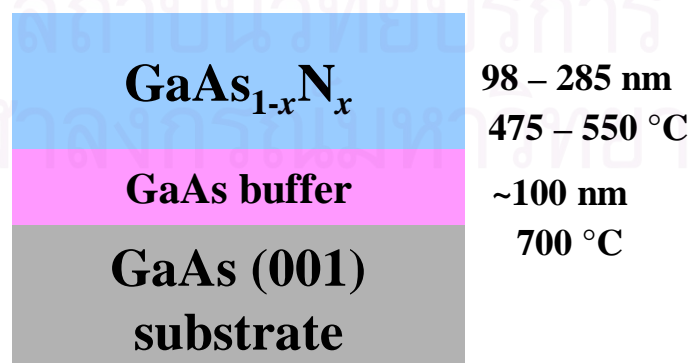
Fig. 2-4 The schematic illustration of GaAs$_{1-x}$N$_x$ sample used in this thesis.

Samples	[DMHy] (μmol/min)	T_g (^{0}C)
MO-0072	500	550
MO-0053	1,000	550
MO-0073	1,500	550
MO-0054	2,000	550
MO-0055	3,000	550
MO-0056	4,000	550
MO-0080	2,000	500
MO-0076	3,000	500
MO-0075	4,000	500
MO-0074	5,000	500
MO-0104	5,000	475

Table 2-3 GaAsN alloy samples used in this studies and the molar flow rates of [DMHy] and the growth temperature (T_g).

GaAs (001) substrates at temperatures ranging from 475 to 550°C. An un-doped GaAs buffer layer of ~100 nm was first grown at 650°C. The substrate temperature was then reduced to 475-550°C for the growth of GaAs$_{1-x}$N$_x$ layers. The [TBAs]/[TMGa] ratio was maintained at 15. The molar flow rates of [TMG] and [TBAs] were fixed at 8.64 and 129.70 μmol/min, respectively. The molar flow rate of [DMHy] was varied in the range of 0 to 5000 μmol/min. Table 2-3 presents samples used in this study and the flow rates of [DMHy] and the growth temperatures. And, the schematic diagram of structure of the GaAs$_{1-x}$N$_x$ sample is displayed in Fig. 2-4.

2.3.2 High resolution X-ray diffraction

High resolution X-ray diffraction (HRXRD) is very powerful technique that is indispensable for crystal structure analysis of the epitaxial films. HRXRD measurements were carried out to determine the strain properties and the N

concentration (x) of the epitaxial GaAs$_{1-x}$N$_x$ films. Both symmetric (004) and asymmetric (115) reflections were measured, to determine the lattice constants of GaAsN layers perpendicular ($a_{\perp}$) and parallel ($a_{//}$) to the GaAs (001) surface. The symmetric and asymmetric reflections are (004) 2ɵ/ω scan and (115) ω/2ɵ scan mapping, respectively. Figure 2-5 shows HRXRD profile (004) of the GaAsN layer on the GaAs (001) substrate. Optimization of 2ɵ/ω scan is done for the Bragg peak of the GaAs substrate as a reference crystal. The GaAsN layer was grown at 550°C and the molar flow rate of [DMHy] was 2000 μmol/min. The narrow GaAsN diffraction peak and Pendellösung fringes are clearly observed. This indicates that the GaAsN epitaxial film has a high crystal quality and coherently grown on the GaAs substrate. The diffraction peak of GaAsN appears with higher value of 2ɵ/ω, This shows that the GaAsN layer has tensile strain. The value of $a_{\perp}$ is estimated from the separation between the GaAs and GaAsN diffraction peaks by the following equation;

$$\text{Bragg's law: } 2d\sin\theta = n\lambda \text{ ; } d_{hkl} = \frac{\lambda}{2\sin\left(\dfrac{2\theta_{hkl}}{2}\right)} \tag{2-4}$$

$$d_{hkl} = \frac{a_{\perp}}{\sqrt{h^2 + k^2 + l^2}} \tag{2-5}$$

From these equations, the value of $a_{\perp}$ is estimated to be 5.612 Å. The thickness of GaAsN layer was calculated by usual formula [25] to be 240.72 nm.

It is well known that the inclination between the asymmetric plane of substrate and that of the epitaxial film is usually observed if the film is subjected to a tetragonal distortion [5]. The angle ψ between the (001) and the (115) planes of strained layer is given by;

$$\psi = \tan^{-1}\left(\sqrt{2} \cdot a_{\perp} / 5 \cdot a_{//}\right) \tag{2-6}$$

If the lattice parameter has cubic symmetry, such as lattice matched layer, fully relaxed layer or GaAs substrate ($a_{\perp} = a_{//}$), $\psi = \tan^{-1}\left(\sqrt{2}/5\right)$. However, ψ for the epitaxial films under the elastic distortion depends on the lattice parameter $a_{\perp}$ and

$a_{//}$. The tilt angle $\Delta\psi$ between the GaAs (115) and the GaAsN (115) planes is represented by;

$$\Delta\psi = \tan^{-1}\left(\sqrt{2}/5\right) - \tan^{-1}\left(\sqrt{2}\cdot a_\perp/5\cdot a_{//}\right) \qquad (2\text{-}7)$$

As seen in Fig 2-6, a single scan cannot determine the diffraction angle with enough accuracy, because the conventional $2\theta/\omega$ scan can measure only one of [115] direction of either substrate or strained layer. Usually, $\Delta\psi$ is determined by two $2\theta/\omega$ curves with the sample rotated by 180° around (115) plane normal [5].
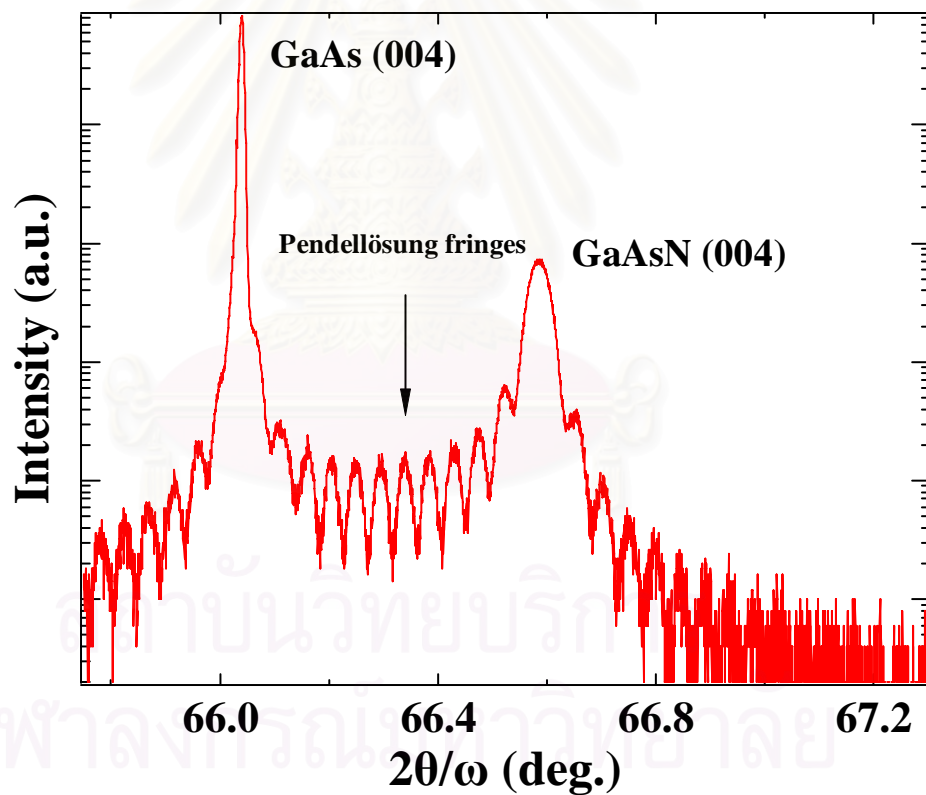
Fig. 2-5 High resolution (004) X-ray diffraction profile of GaAsN layer on GaAs (001) substrate. The GaAsN layer grown at 550°C and the flow rate of DMHy is 2000 μmol/min.
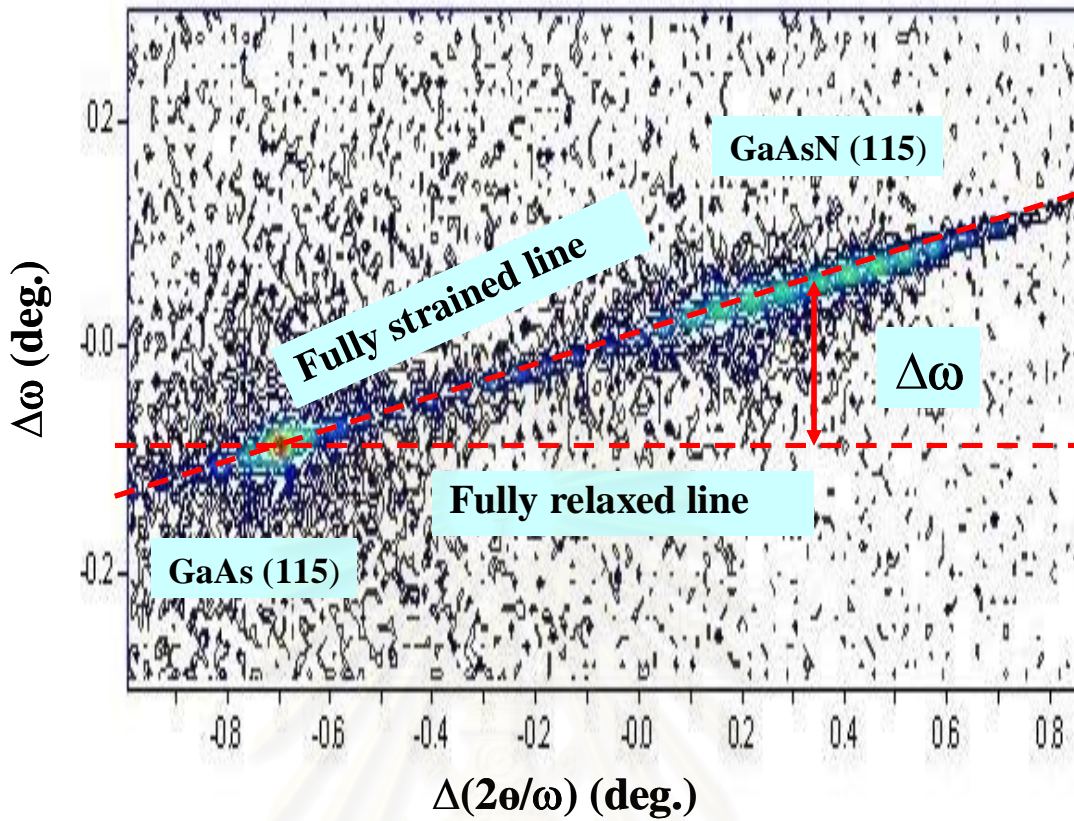
Fig. 2-6 (115) HRXRD map of the GaAsN layer grown on GaAs. The tilt angle $\Delta\psi$ between the GaAs (115) and the GaAsN (115) planes is 0.108°.

Figure 2-6 presents a typical $(2\theta/\omega)$ - $\Delta\omega$ mapping around the (115) diffraction peaks. Both the diffraction peaks from the GaAs (115) and the GaAsN (115) planes are directly observed. The offset $\Delta\omega$ of the separation between the GaAs and GaAsN peaks is estimated to be 0.108°. Thus the tilt angle $\Delta\psi$ between the GaAs (115) and the GaAsN (115) planes is 0.108°. The value of $a_{//}$ calculated using Eq.(2-7) is 5.653 Å, which corresponds to the lattice constant of GaAs. This result implies that the GaAsN layer was coherently grown on the GaAs substrate.

The N concentration (x) in GaAs$_{1-x}$N$_x$ can be estimated from the unstrained lattice constant, a_0, expressed by

$$a_0 = \frac{2C_{12}a_{//} + C_{11}a_{\perp}}{2C_{12} + C_{11}} \tag{2-8}$$

$$a_0 = x\, a_{GaN} + (1 - x)\, a_{GaAs} \tag{2-9}$$

$$C_{11} = \frac{x a_{GaN} C_{11}^{GaN} + (1 - x) a_{GaAs} C_{11}^{GaAs}}{a_0} \tag{2-10}$$

$$C_{12} = \frac{x a_{GaN} C_{12}^{GaN} + (1 - x) a_{GaAs} C_{12}^{GaAs}}{a_0} \tag{2-11}$$

where C_{11} and C_{12} are the elastic constants of GaAs$_{1-x}$N$_x$. a_{GaN} and a_{GaAs} are the lattice constants of the unstrained cubic-GaN and GaAs, respectively. These four equations were used to determine the N concentration in a series of the GaAsN epitaxial films with different [DMHy] flow rates [10].

2.3.3 Raman scattering spectroscopy

When the monochromatic high frequency laser light is incident on the sample, the frequency of the scattered light differs from that of the incident light by the frequency of an optical phonon, the scattering process is called Raman scattering. Inelastic scattering of light by molecular vibrations was first reported by Chandrasekhara Venkata Raman. In 1930 Raman was awarded the Nobel prize for his discovery of Raman scattering [21]. In Raman scattering, the incident light beam is scattered with relatively large frequency shift independent of the scattering angle. The Raman spectrum has Stokes and anti-Stokes branches corresponding to the emission and absorption, respectively.

The frequencie (ω) and wavevectors (k) for the first-order Raman scattering are

$$\omega_i = \omega_s \pm \omega \tag{2-12}$$

$$k_i = k_s \pm k \tag{2-13}$$

where ω_i, k_i refer to the incident photon; ω_s, k_s refer to the scattered photon; and ω, k refer to the phonon created or destroyed in the scattering event. In the second-order

Raman scattering, two phonons are involved in the inelastic scattering of the photon [20]. For two different phonons, peaks with Raman frequencies $\omega_a + \omega_b$ and $\omega_a - \omega_b$ are referred to as the combination and difference modes, respectively, where ω_a and ω_b are the frequencies of the two phonons involved. If the two phonons are identical, the resultant two-phonon Raman peak is called an overtone [21]. Fig. 2-7 presents Stokes and anti-Stokes branches of Raman spectrum in first-order Raman scattering.

Stokes

$$\omega_i = \omega_s + \omega$$

$$k_i = k_s + k$$

Anti-Stokes

$$\omega_i = \omega_s - \omega$$

$$k_i = k_s - k$$
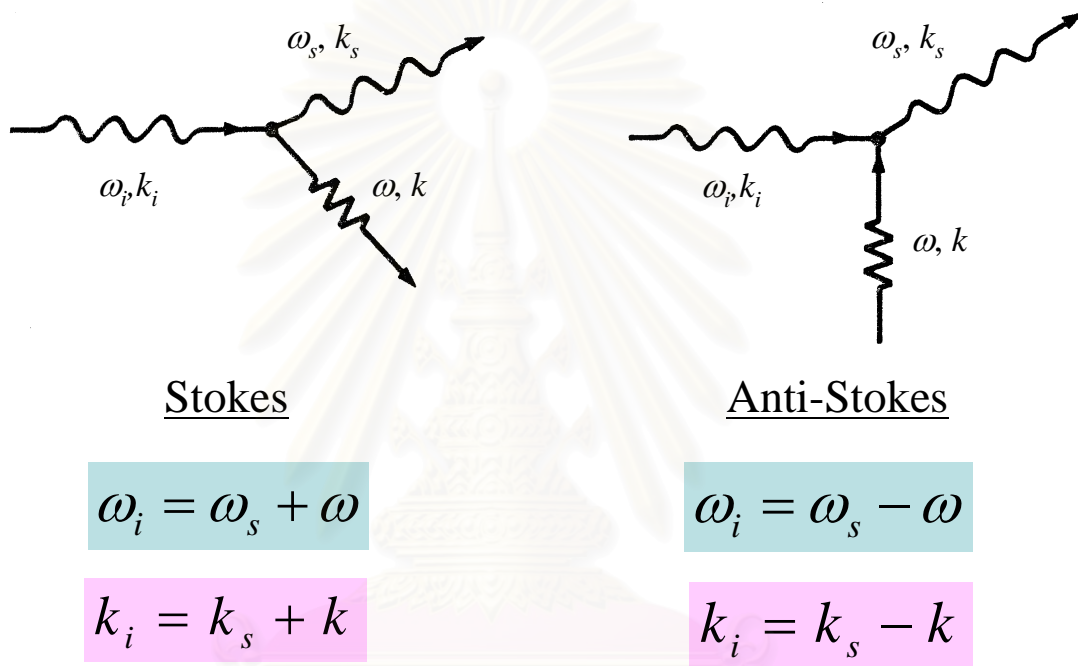
Fig. 2-7 Schematic representation of the first-order Raman scattering by optical phonon.

The simplest scattering geometry is the backscattering. The wavevector k_i and k_s are antiparallel to each other. From wavevector conservation, the wavevector k of the phonon must be along the [001] direction also for backscattering from a (001) surface. Raman scattering by the TO phonon is forbidden in this backscattering geometry. The scattering geometry is written as $k_i(e_i, e_s)k_s$, where k_i and k_s are the directions of the incident and scattered photons; e_i and e_s are the polarizations of the incident and scattered photons. Thus, the scattering geometries for backscattering from the (001) surface of a GaAs$_{1-x}$N$_x$ crystal are $z(x, y)\bar{z}$ or $z(y, x)\bar{z}$.

The Raman scattering focus is on atomic vibration, wavenumber unit (cm^{-1}) is standard for vibrational studies. Wavenumber is the reciprocal of the wavelength of the light. Since the phonon frequency is equal to the difference between the incident photon frequency and the scattered photon frequency, this difference is referred to as the Raman frequency or Raman shift. Raman spectra are usually plots of the intensity of the scattered radiation versus the Raman shift in wavenumber unit (cm^{-1}).

2.3.4 Fourier transform infrared spectroscopy

Fourier transform infrared (FTIR) spectroscopy is an analytical technique used to investigate many aspects of materials including bandgap energy. This technique measures the absorption of various infrared light wavelengths by the material of interest. These infrared absorption bands identify specific molecular components and structures. Because the material absorbs infrared energy at specific frequency, the bandgap energy of the semiconductor materials can be determined by the spectral location of its infrared (IR) absorption. FTIR spectrometer offers speed and sensitivity impossible to achieve with earlier wavelength-dispersive instruments.

2.3.5 Photoluminescence spectroscopy

When the sample is illuminated by light, the sample absorbed photons of energy higher than bandgap and emitted photons of energy lower than the excitation photons, this optical process is called photoluminescence (PL). The emitted light in PL corresponds to the characteristic electronic transition energy of the samples. PL emission band occurs at a position fixed by transition energy; it does not shift with laser photon energy $h\upsilon_L$. This is in contrast to a Raman emission line, which tracks with $h\upsilon_L$ because it is the small redshift that corresponds to crystal excitation energy [22].

CHAPTER III

COMPOSITIONAL INVESTIGATION
OF GaAsN ALLOY LAYERS

3.1 Introduction

It is known that the accurate determination of the N concentration in $GaAs_{1-x}N_x$ is very important, in order to control the bandgap and quality of the $GaAs_{1-x}N_x$ films. High resolution X-ray diffraction (HRXRD) has been widely used to analyze structural quality and determine N concentrations of the $GaAs_{1-x}N_x$ films. In this chapter, the $GaAs_{1-x}N_x$ alloy films ($0 \leq x \leq 0.055$) have been studied by HRXRD.

The N content in the $GaAs_{1-x}N_x$ films were determined from a symmetrical (004) and an asymmetrical (115) HRXRD measurements, assuming a linear dependence of lattice constant on the N concentration.

3.2 HRXRD measurements

High resolution X-ray diffraction (HRXRD) measurements were done at, Department of Advanced Materials Science, The University of Tokyo, and Scientific and Technological Research Equipment Centre, Chulalongkorn University (the Bruker-AXS D8 DISCOVER). HRXRD instrument set up are shown in Fig. 3-1. HRXRD measurements were performed using a copper target ($K\alpha_1 = 1.5406$ Å) as the radiation source. A detail about HRXRD method was described in previous chapter. In addition, we used the simulation software using "the dynamic theory" to study the thickness of the $GaAs_{1-x}N_x$ layers as well as the N concentration.
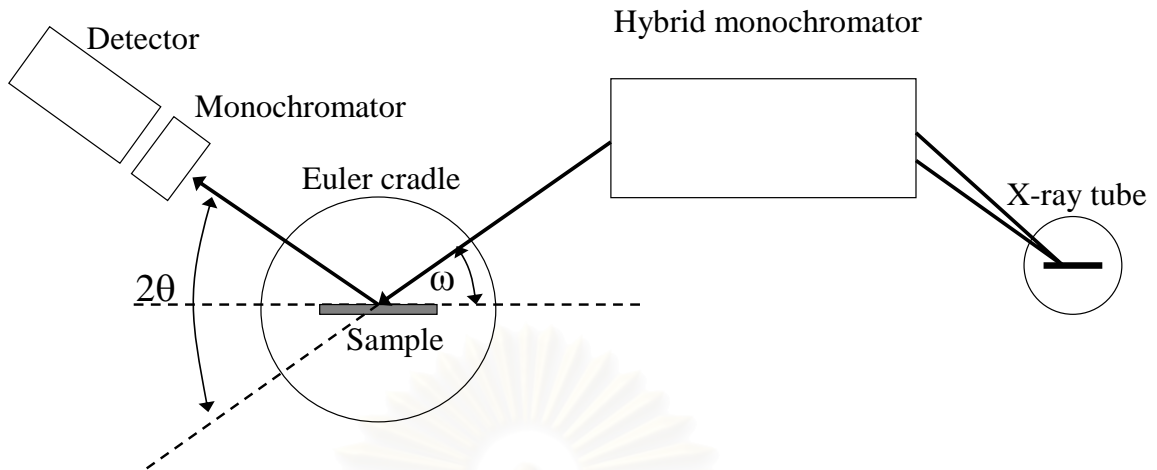
Fig. 3-1 High-resolution X-ray diffraction (HRXRD) instrument set up.

3.3 Results and discussion

All the GaAs$_{1-x}$N$_x$ films used in this study were investigated by HRXRD in order to determine the N concentration (x_{XRD}) and verify the structural quality. Figure 3-2 shows a symmetric (004) HRXRD scans obtained from a set of the GaAs$_{1-x}$N$_x$ films with different N concentrations. As shown in the figure, compared with GaAs, the peak shift to the higher diffraction angles was clearly observed with increasing N concentration, indicating the reduction of a lattice constant ($a_\perp$) normal to the (001) surface with the N incorporation. The narrow diffraction peaks and the clear Pendellösung fringes indicate that GaAsN films with high crystal quality were coherently grown on the GaAs substrate. Table 3-1 represents the value of $a_\perp$ of the GaAs$_{1-x}$N$_x$ films, which estimated from the separation between the GaAs and GaAsN diffraction peaks, and the thickness of the GaAs$_{1-x}$N$_x$ films calculated from the Pendellösung fringes using standard formula [25]. The reciprocal lattice mapping of an asymmetrical (115) reflection is shown in Fig. 3-3 for the GaAs$_{1-x}$N$_x$ films with N content of $x_{\mathrm{XRD}} = 0.0275$. It can be seen that the diffraction peaks of GaAs and GaAsN located at the fully strained line. This suggests that the GaAs$_{1-x}$N$_x$ film was coherently strained grown on the GaAs substrate. The offset $\Delta\omega$ of the separation between the GaAs and GaAsN peaks is estimated to be 0.108°. Thus the tilt angle $\Delta\psi$

between the GaAs (115) and the GaAsN (115) plane is 0.108^{o}. The value of $a_{//}$ calculated using Eq. (2-7) is 5.653 Å, which corresponds to the lattice constant of GaAs. These results confirm that the GaAsN film was coherently strained grown on the GaAs substrate.
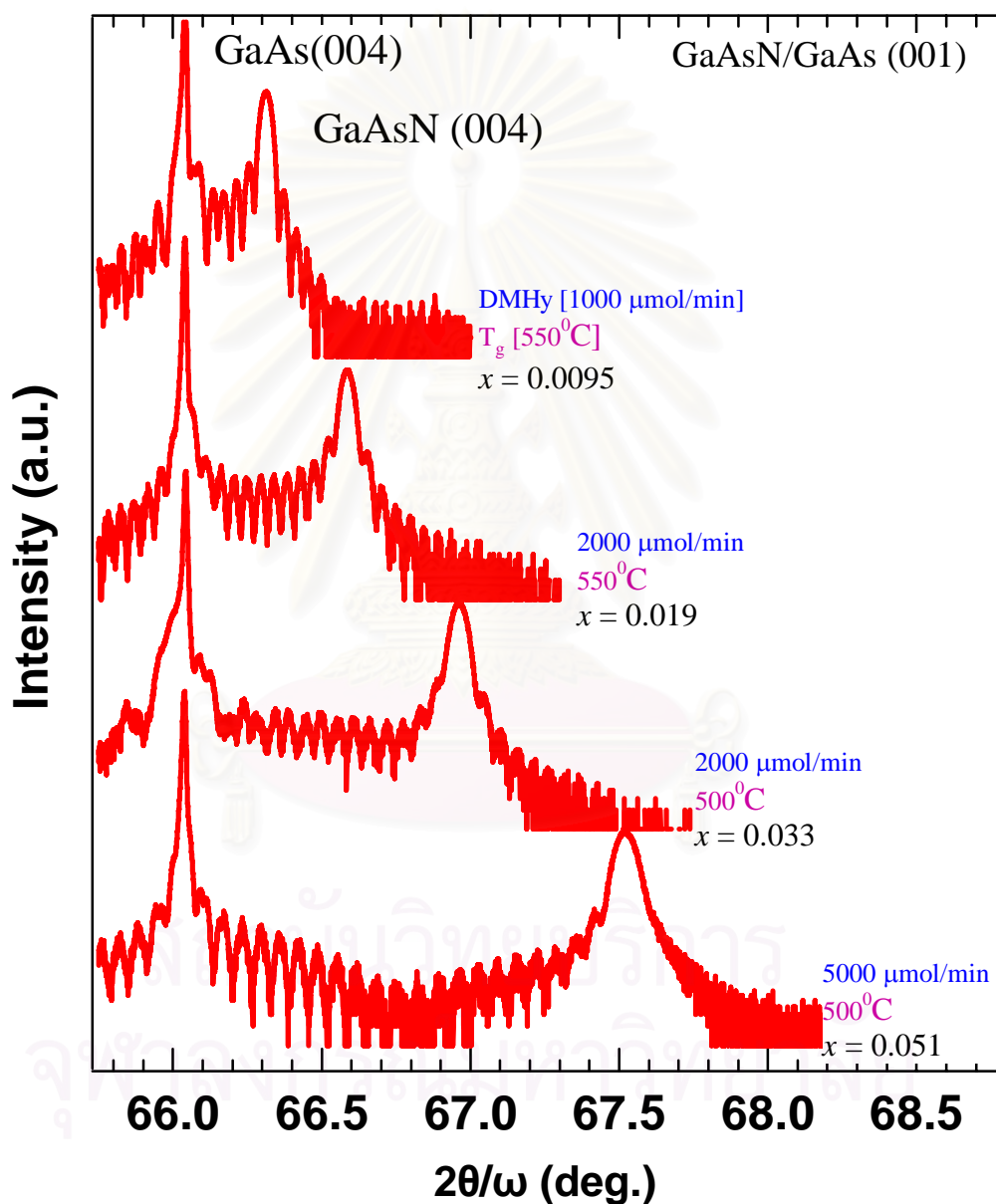
Fig. 3-2 High-resolution (004) X-ray diffraction profiles of GaAs$_{1-x}$N$_x$ layers grown on the GaAs (001) substrates.

Samples	$a_\perp$ (Å)	Films thickness (nm)
MO-0072	5.6443	248.5
MO-0053	5.6324	248.5
MO-0073	5.6219	285.3
MO-0054	5.6120	240.7
MO-0055	5.6019	202.7
MO-0056	5.5936	214.0
MO-0080	5.5844	214.0
MO-0076	5.5657	171.2
MO-0075	5.5519	197.5
MO-0074	5.5435	167.5
MO-0104	5.5330	97.5

Table 3-1 The lattice constant ($a_\perp$) of the GaAs$_{1-x}$N$_x$ films, that estimated from the separation between the GaAs and GaAsN diffraction peaks, and the thickness of the GaAs$_{1-x}$N$_x$ films calculated using standard formula.
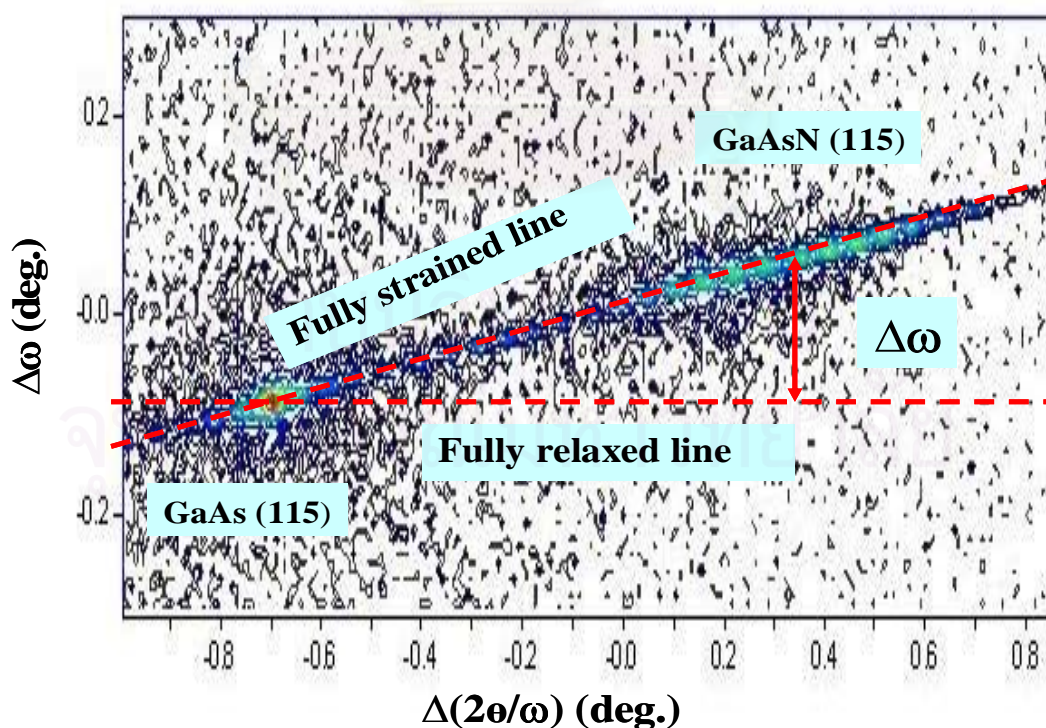
Fig 3-3 The reciprocal lattice mapping of an asymmetrical (115) reflection for the GaAs$_{1-x}$N$_x$ films with N content of $x_{\text{XRD}} = 0.0275$.

Figure 3-4 shows the reciprocal lattice mapping of an asymmetrical (115) reflection for the GaAs$_{1-x}$N$_x$ films with N concentration of x_{XRD} = 0.051. This confirms that such high N-containing GaAsN layer is also coherently strained and is of good epitaxial quality. These results are an evidence of high crystal quality films with higher N contents up to ~ 5%, obtained by the enhanced incorporation of N at lower growth temperatures (~ 500°C) [24].

The N concentration, and the lattice constant ($a_\perp$) of GaAs$_{1-x}$N$_x$ films are listed in table 3-2. As shown in this table, the value of $a_\perp$ decreases when the N concentration increases. This indicates the tensile strain in the GaAs$_{1-x}$N$_x$ films increase with N incorporation. The Δx_{XRD} that displayed in this table estimated from full width at half maximum (FWHM) of the GaAs and GaAsN diffraction peaks, indicating higher accurate determination of the N concentration.
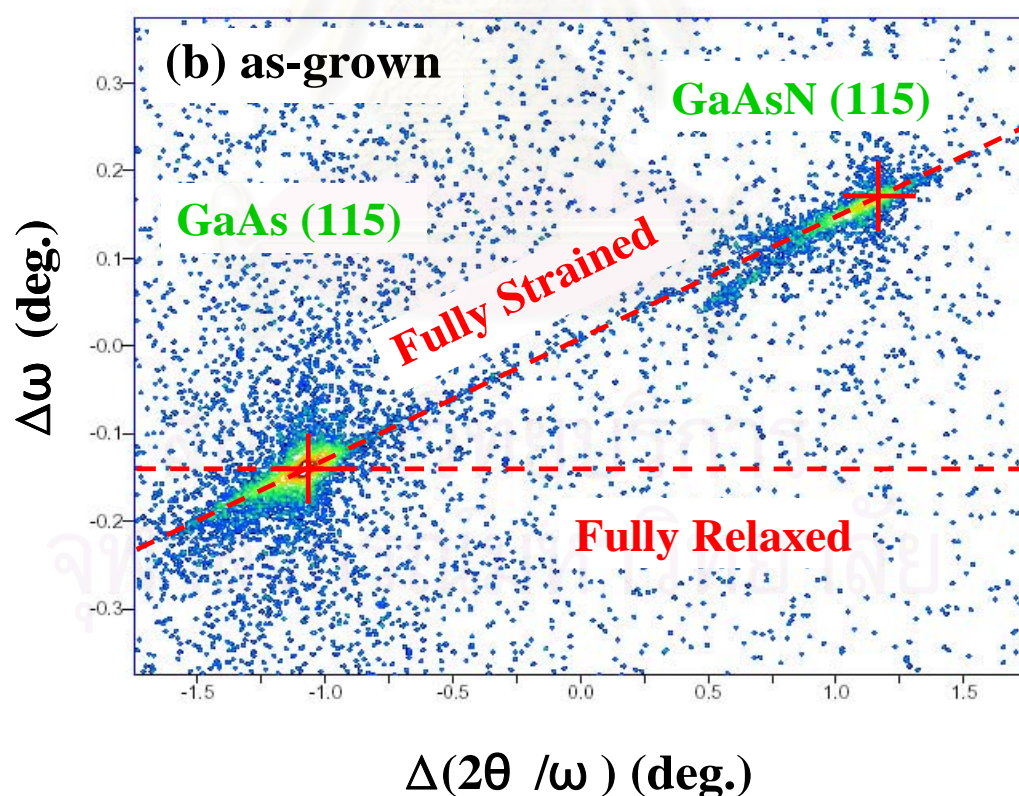
Fig 3-4 The reciprocal lattice mapping of an asymmetrical (115) reflection for the GaAs$_{1-x}$N$_x$ films with N concentration of x_{XRD} = 0.051.

Samples	$a_\perp$ (Å)	x_{XRD}	Δx_{XRD}
MO-0072	5.6443	0.0050	0.0003
MO-0053	5.6324	0.0095	0.0003
MO-0073	5.6219	0.0150	0.0005
MO-0054	5.6120	0.0190	0.0007
MO-0055	5.6019	0.0235	0.0009
MO-0056	5.5936	0.0275	0.0009
MO-0080	5.5844	0.0330	0.0005
MO-0076	5.5657	0.0410	0.0012
MO-0075	5.5519	0.0480	0.0009
MO-0074	5.5435	0.0510	0.0012
MO-0104	5.5330	0.0550	0.0012

Table 3-2 The N concentration (x_{XRD}), and normal lattice constant ($a_\perp$) of the GaAs$_{1-x}$N$_x$ films

In addition, to confirm the above results, the simulation software was used to determine the N concentration and thickness of the GaAs$_{1-x}$N$_x$ alloy layers. The parameters necessary for this simulation are strain, thickness, and N concentration of GaAs$_{1-x}$N$_x$ alloy layers. Figure 3-5 displays the High-resolution (004) X-ray diffraction profiles of GaAs$_{1-x}$N$_x$ layers grown on the GaAs (001) substrates represented by the red solid lines, and the simulation profiles represented by the blue dashed lines. It is clearly seen in the figure that the (004) HRXRD profiles agree well with the simulation profiles. These results confirm the accurate determination of both the thickness and the N concentration of GaAs$_{1-x}$N$_x$ layers, which are analyzed using HRXRD.

The N concentrations and the thicknesses of the GaAs$_{1-x}$N$_x$ alloy layers which were determined by HRXRD measurements and simulation given in table 3-3. As shown in this table, a good agreement between results from HRXRD measurement and simulation was obtained.
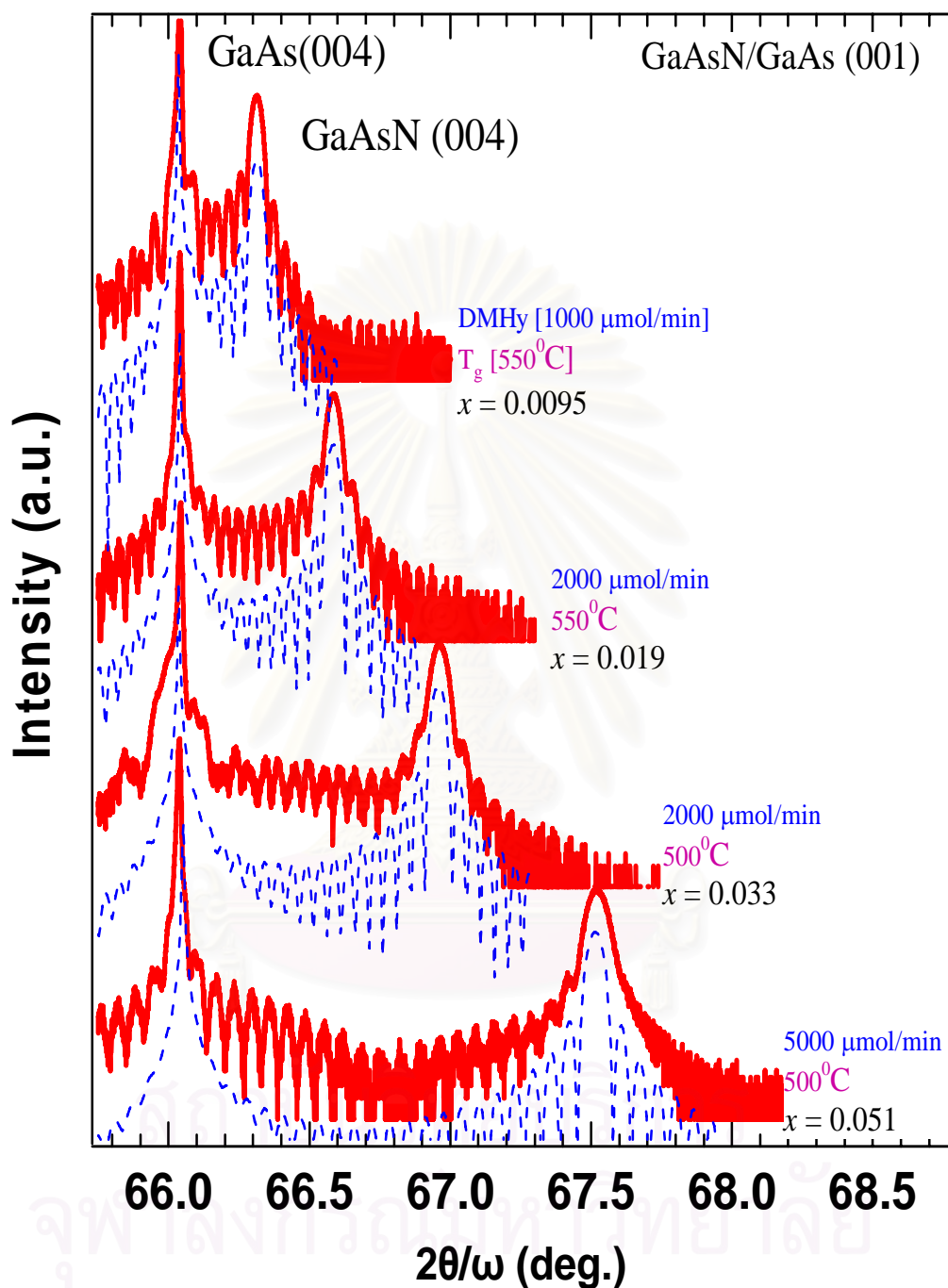
Fig 3-5 The High-resolution (004) X-ray diffraction profiles of the $GaAs_{1-x}N_x$ layers grown on the GaAs (001) substrates with different N concentrations, and the simulation profiles. Red solid lines and blue dashed lines represent the HRXRD, and the simulation profiles, respectively.

Samples	High resolution X-ray diffraction			Simulation	
	x_{XRD}	Δx_{XRD}	Films thickness (nm)	x_{Sim}	Films thickness (nm)
MO-0072	0.0050	0.0003	248.5	0.0050	248
MO-0053	0.0095	0.0003	248.5	0.0095	248
MO-0073	0.0150	0.0005	285.5	0.0150	285
MO-0054	0.0190	0.0007	240.7	0.0190	241
MO-0055	0.0235	0.0009	202.7	0.0235	203
MO-0056	0.0275	0.0009	214.0	0.0275	214
MO-0080	0.0330	0.0005	214.0	0.0330	214
MO-0076	0.0410	0.0012	171.2	0.0410	171
MO-0075	0.0480	0.0009	197.5	0.0480	198
MO-0074	0.0510	0.0012	167.5	0.0510	167
MO-0104	0.0550	0.0012	97.5	0.0550	98

Table 3-3 The N concentrations in $GaAs_{1-x}N_x$ alloy layers which determined by HRXRD measurement (x_{XRD}) and simulation (x_{Sim}). Also, the thicknesses of the $GaAs_{1-x}N_x$ layers were shown.

3.4 Summary

The structural quality and the N concentrations of the $GaAs_{1-x}N_x$ alloy alloy films ($0 \leq x \leq 0.055$) have been investigated by high resolution X-ray diffraction (HRXRD). It has clearly observed that the $GaAs_{1-x}N_x$ alloy films which high N contents up to 0.055, are coherently strained and good epitaxial quality. The N concentrations in $GaAs_{1-x}N_x$ and the thickness of $GaAs_{1-x}N_x$ films are determined by HRXRD measurement and simulation. The results from HRXRD measurement have a good agreement with the results obtained from simulation. This confirms that the N concentrations and the thickness of $GaAs_{1-x}N_x$ alloy layers estimated by the HRXRD measurement are accurate.

CHAPTER IV

RAMAN SCATTERING OF GaAsN ALLOY LAYERS

4.1 Introduction

Raman spectroscopy is a powerful technique to obtain information on crystal structure through measuring the vibrations of the crystal lattice. Raman spectra provide a sensitive tool for studying the impurity incorporation in such structure and the structural defects [6]. It is known that N-related local vibrational mode (LVM) absorption is directly proportional to the N concentration in $GaAs_{1-x}N_x$. Seong et al. compared the N concentrations in $GaAs_{1-x}N_x$ determined by Raman spectroscopy technique (x_{Raman}) with those determined by X-ray diffraction (XRD) (x_{XRD}) [4]. They demonstrated that that x_{Raman} exhibits a linear dependence on x_{XRD} for $x_{XRD} < 0.03$ and some deviation from the linear dependence for $x_{XRD} > 0.03$. In this chapter, we first review the results of Raman spectroscopic studies on the local bonding of N in $GaAs_{1-x}N_x$ with N concentrations up to $x_{XRD} = 0.055$. Secondly, we describe the N concentration dependence of the LVM in $GaAs_{1-x}N_x$ films.

4.2 Raman Scattering Measurements

Micro-Raman scattering used in this study were done with the Renishaw ramascope RM1000 at The Gem and Jewelry Institute of Thailand, Faculty of Science, Chulalongkorn University. Raman spectra were recorded at room temperature in backscattering geometry on the (001) growth surface of samples. The scattering configuration of $z(x, y)\bar{z}$ is used, where x, y and z correspond to the (100), (010) and (001) crystal directions, respectively. The spectral range was set at the wave number of 250 - 700 cm^{-1}. The Ar^{+} 514.5-nm laser line was used as an excitation light source. The excitation laser beam was focused by a microscope lens system yielding a spot size ~ 2 - 4 μm in diameter. Raman spectroscopy set up is shown in Fig. 4-1.
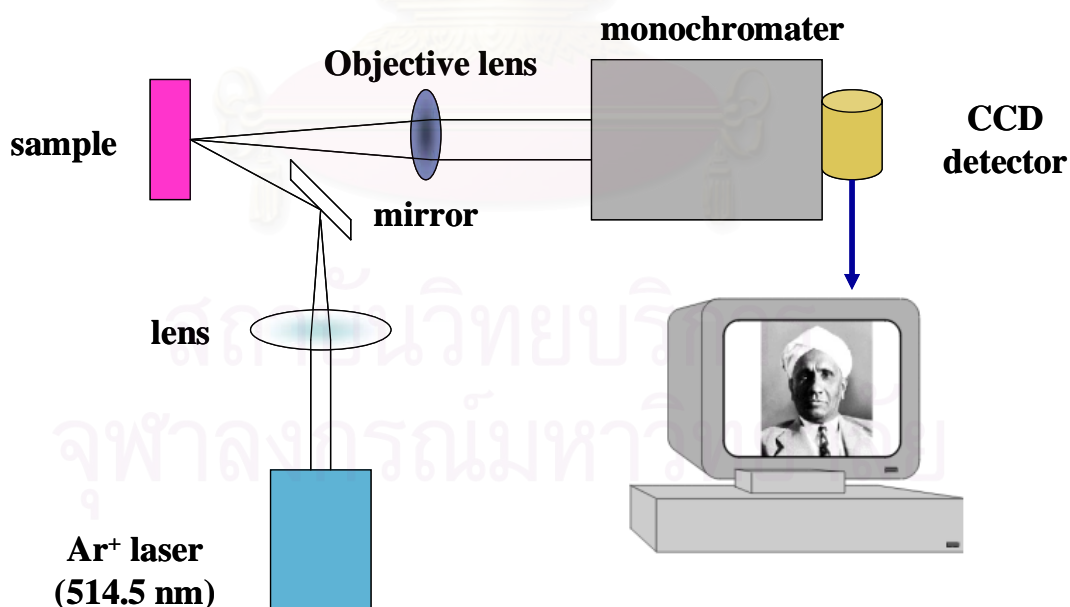
Fig. 4-1 The experimental set up for Raman scattering measurements.

In the case of GaAs, the optical penetration depth (d = 1/α ; where α is the absorption coefficient) is about 100 nm for a photon energy of 2.41 eV (or 514.5-nm wavelength, corresponding to the green line of Ar$^+$ laser) [26]. Thus, Raman scattering with incident light wavelength 514.5 nm is a great technique to study the regions of thin GaAsN films with thickness as thin as 100 nm. The number of samples used in this study are 11 samples. Raman spectra were recorded from five different areas (five spots) for each sample.

4.3 Results and discussion

Figure 4-2 shows a typical Raman spectrum recorded at room temperature (RT) for the GaAs$_{1-x}$N$_x$ film with N content of x_{XRD} = 0.041. Raman spectrum shows the transverse optical (TO) and longitudinal (LO) phonon modes of GaAs, along with a single N-related LVM. The GaAs-LO line width is narrow, indicating high crystal quality. It is known that the Raman spectrum taken from the GaAs$_{1-x}$N$_x$ layer shows the GaN-like LO phonon mode, namely N-related LVM, at 471 cm^{-1} [27-29].

A sequence of room temperature Raman spectra taken from the GaAs$_{1-x}$N$_x$ films with N contents up to x = 0.051 is displayed in Fig. 4-3. The Raman intensity is normalized with respect to the GaAs-LO Raman intensity ($I_{GaAs-LO}$) for each sample and the base lines are subtracted. In the N-incorporating films, a single N-related LVM is observed at around 467 - 475 cm^{-1}. This mode has been attributed to the vibration associated with isolated N atoms at arsenic site [29]. It was observed that the normalized N-related LVM Raman intensity was enhanced with increasing N concentration. As expected, the deterioration of the second order Raman features of GaAs near 513 and 540 cm^{-1} [4] due to the N incorporation were clearly observed as

shown Fig. 4-3. A gradual blue shift of the Raman frequency of the N-related LVM (ω_{LVM}) was also observed. In Fig. 4-4, the best fit yields $I_{LVM}/(I_{LVM}+I_{GaAs-LO}) = (1.44 \pm 0.04)\, x_{XRD}$. And, the best fit of $\omega_{LVM} = (467.75 \pm 0.59) + (118.70 \pm 17.36)\, x_{XRD}$ is shown in Fig.4-5. It found that the ω_{LVM} exhibits linearly depend on x_{XRD}, because of the effects of alloying and strain [30].
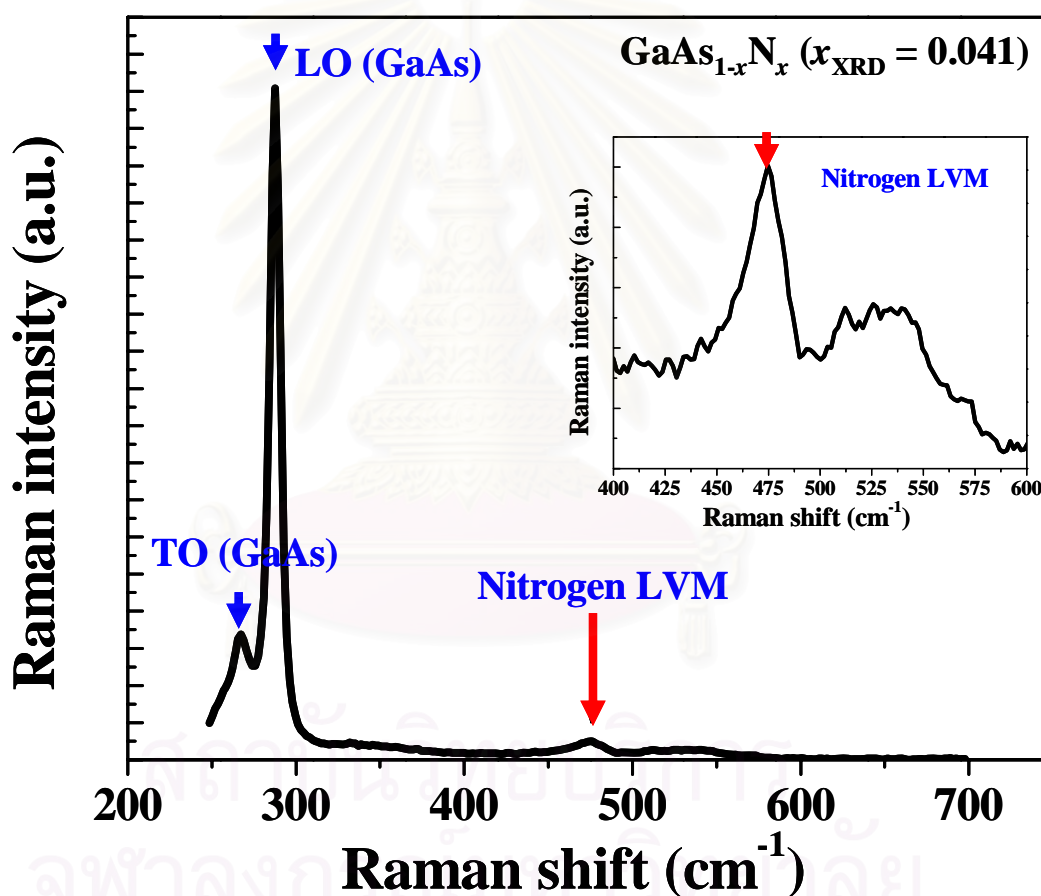
Fig. 4-2 Raman spectrum of GaAs$_{1-x}$N$_x$, for N concentration of $x_{XRD} = 0.041$, excited with Ar$^+$ 514.5-nm laser line at room temperature in backscattering geometry on the (001) growth surface of samples.
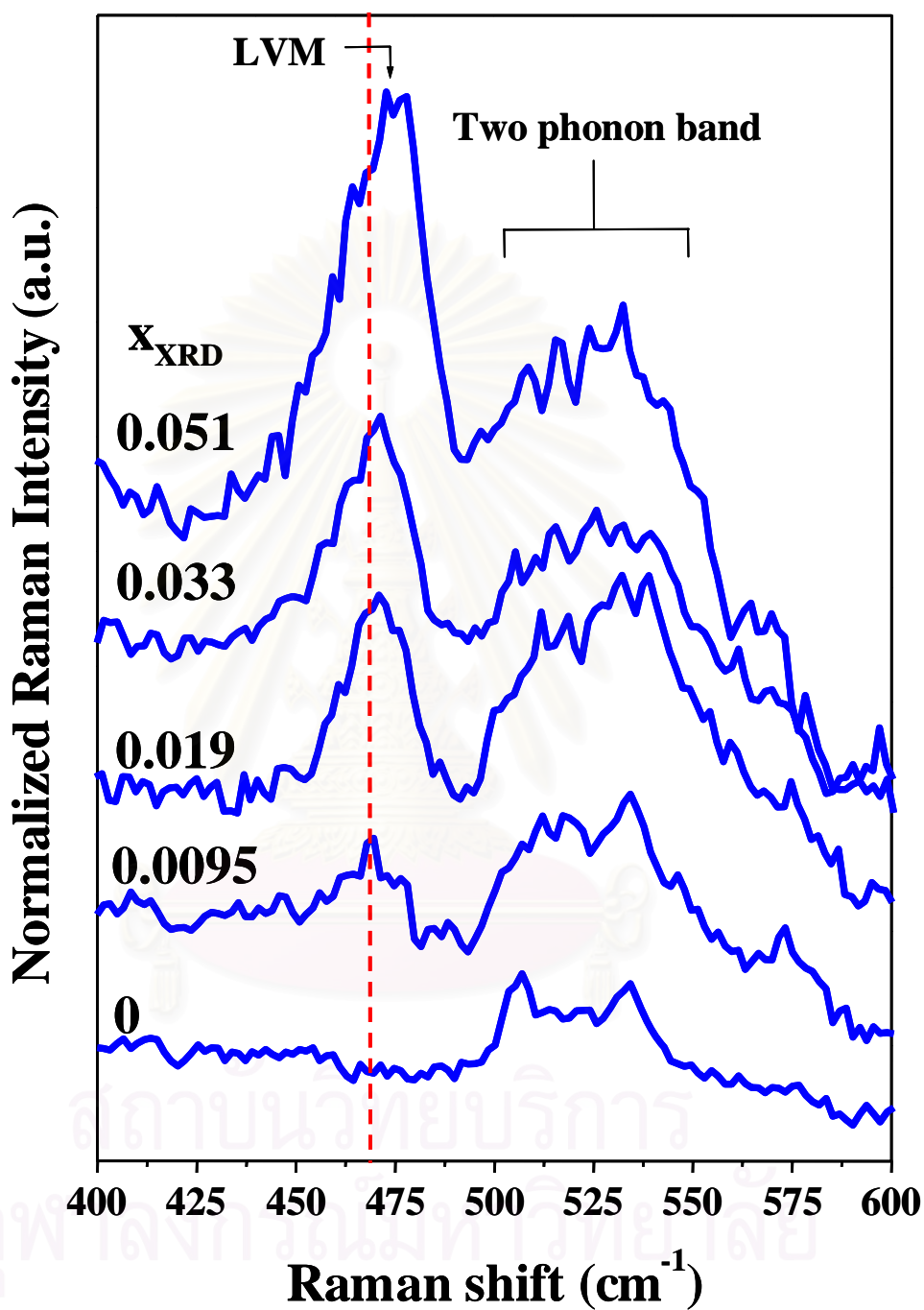
Fig. 4-3 Raman spectra of GaAs$_{1-x}$N$_x$ with different N concentrations of $x_{XRD} = 0$, 0.0095, 0.019, 0.033 and 0.0510, excited with Ar$^+$ 514.5-nm laser line at room temperature.
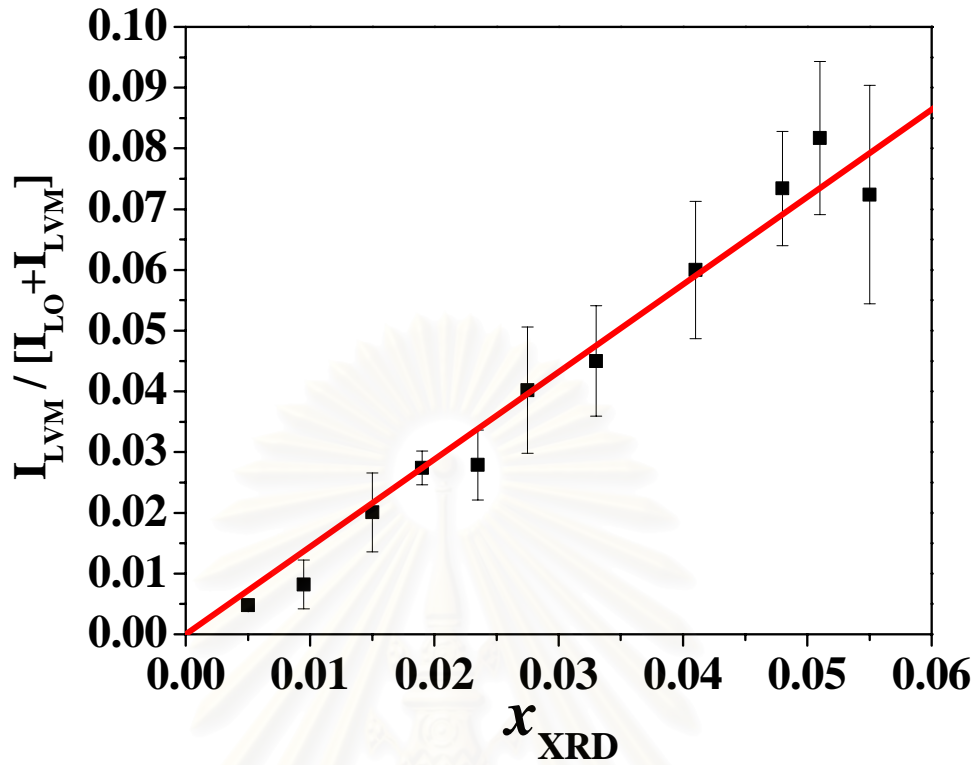
Fig. 4-4 The relationship between the $I_{LVM}/(I_{LVM}+I_{GaAs-LO})$ ratio and the N concentration (x_{XRD}) in the GaAs$_{1-x}$N$_x$ alloy films. The data points are averaged data, which were obtained from five spots on the sample. Error bars indicate the standard deviation.

The full width at half maximum (FWHM) of N-related LVM as a function of x_{XRD} are presented in Fig. 4-6. It is seen that, the FWHM of N-related LVM increase with the N concentration, due to the incorporation of N and strain [29].

It is known that the integrated intensity of GaAs-LO ($I_{GaAs-LO}$) in GaAs$_{1-x}$N$_x$ is proportional to the As concentration and that of N-related LVM (I_{LVM}) is proportional to the N concentration. Then x_{Raman} from the Raman scattering measurements can be calculated as follows [4];

$$x_{Raman} = \frac{I_{LVM}}{f \cdot I_{GaAs-LO} + I_{LVM}} \tag{4-1}$$

where f represents the relative N-related LVM oscillator strength with respect to that of the GaAs-LO phonon. The integrated Raman intensities of GaAs-LO and N-related LVM obtain by subtracted the base lines and then fit the spectrum with Lorentzian oscillator. Figure 4-7 shows the integrated Raman intensities of GaAs-LO and N-related LVM of GaAs$_{1-x}$N$_x$ with $x_{XRD} = 0.041$. From Eq. (1), we can said the data points in Fig. 4-4 using $f = 1$ that assuming equal oscillator strengths for Ga-As and Ga-N modes [4]. But the difference between x_{Raman} and x_{XRD} increases with the N concentration indicates that oscillator strength for the Ga-N mode stronger than that of the Ga-As mode.
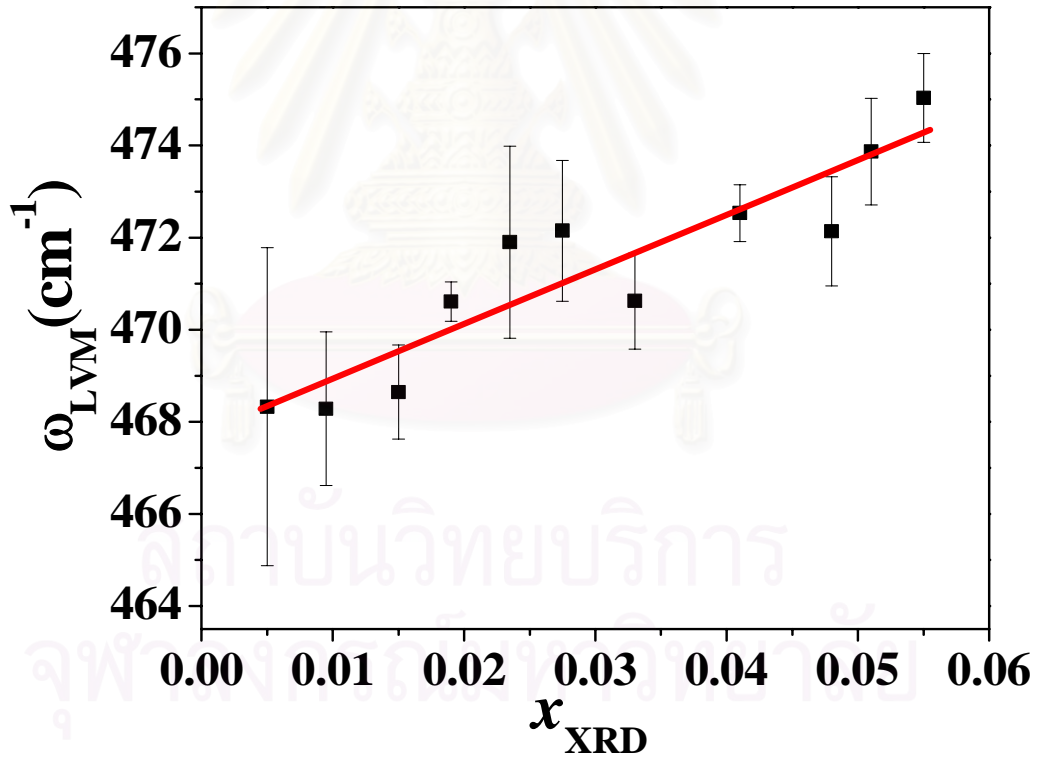
Fig. 4-5 The relationship of the Raman frequency of the N-related LVM (ω_{LVM}), and the N concentration (x_{XRD}) in the GaAs$_{1-x}$N$_x$ alloy films. The data points are averaged data, which were obtained from five spots on the sample. Error bars indicate the standard deviation.
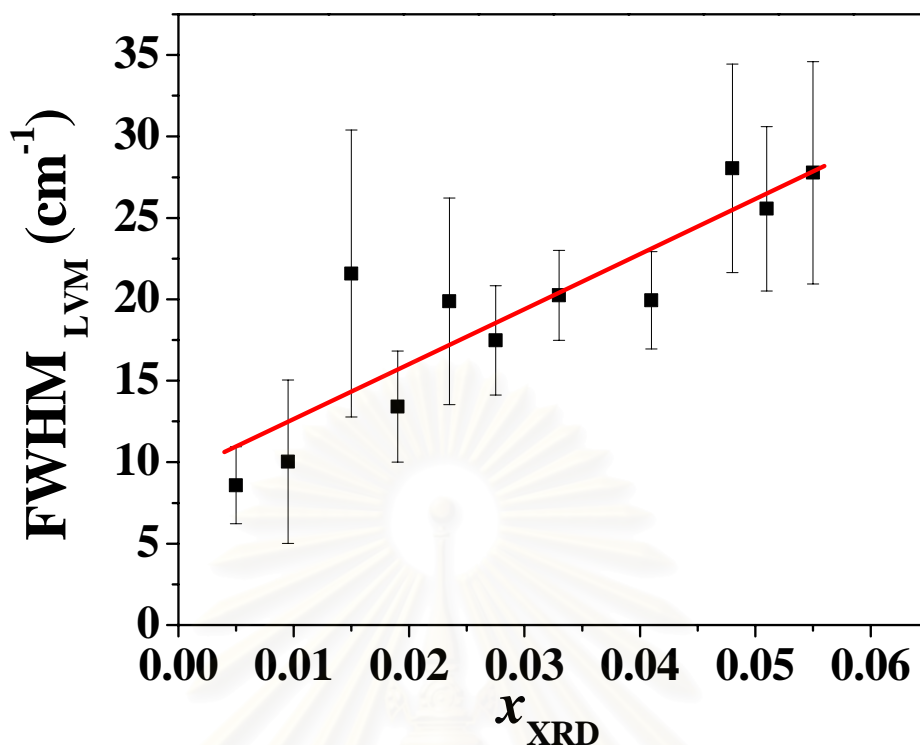
Fig. 4-6 The FWHM of N-related LVM, as a function of x_{XRD}. The solid line gives the best fit, $FWHM_{LVM} = (9.26 \pm 2.03) + (337.83 \pm 59.80)x_{XRD}$. The data points are averaged data, which were obtained from five spots on the sample. Error bars indicate the standard deviation.
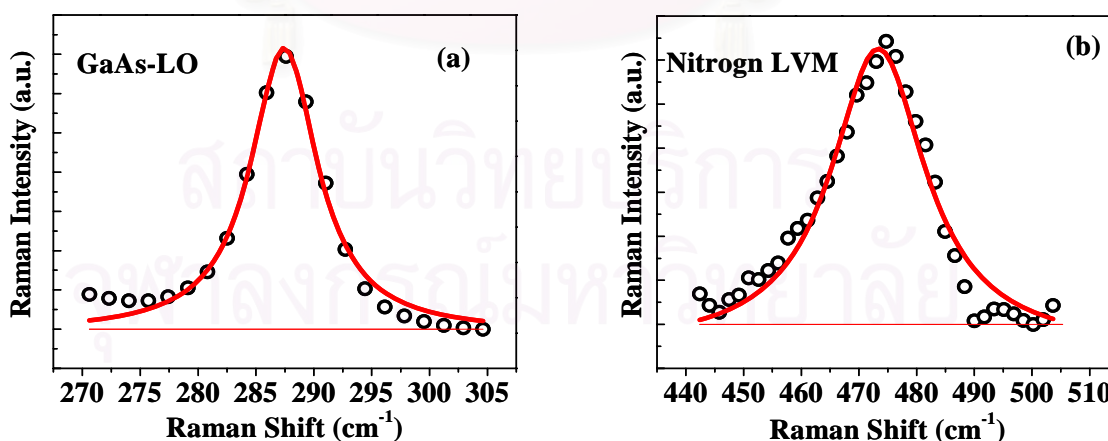
Fig. 4-7 The integrated intensities of (a) GaAs-LO and (b) N-related LVM of $GaAs_{1-x}N_x$ films with $x_{XRD} = 0.041$, analyzed using Lorenzian curve fitting after base-line corrections.

The average x_{Raman} calculated using the Eq. (4-1) as a function of x_{XRD} is displayed in Fig. 4-8. The data points were obtained using $f = 1.4$, giving the best fit ($x_{Raman} = x_{XRD}$) for the N contents up to $x_{XRD} = 0.055$. The small error bars shown in Fig. 4-8 indicate the high alloy uniformity of $GaAs_{1-x}N_x$ layers used in this study. Table 4-1 shows x_{XRD} and x_{Raman} calculated using $f = 1$ and 1.4 for each $GaAs_{1-x}N_x$ sample. It is seen that the x_{Raman} using $f = 1.4$ is approximately equal to x_{XRD}.
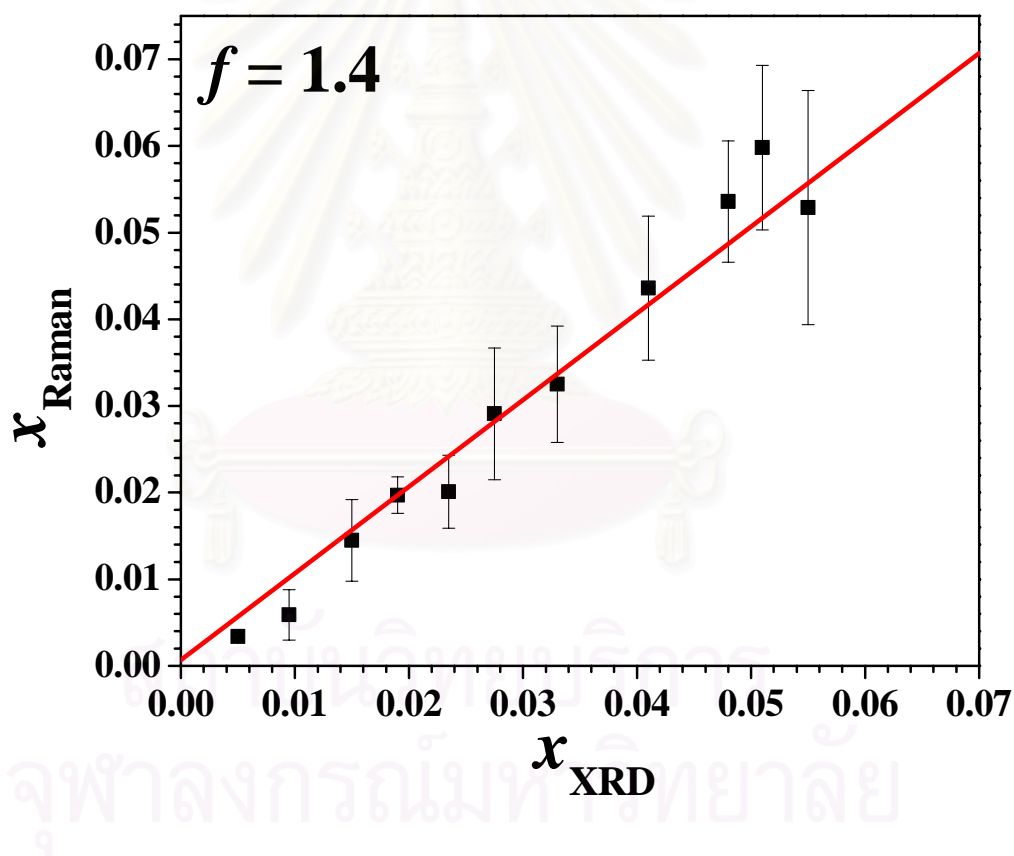
Fig. 4-8 The N concentrations, x_{Raman}, calculated using Eq. (1) as a function of the N concentration determined by HRXRD measurement, x_{XRD}. The solid line represents a linear fit, $x_{Raman} = x_{XRD}$. The data points are averaged data, which were obtained from five spots on the sample. Error bars indicate the standard deviation.

Samples	x_{XRD}	Δx_{XRD}	x_{Raman}			
			$f = 1$	sd	$f = 1.4$	sd
MO-0072	0.0050	0.0003	0.0048	0.0009	0.0034	0.0006
MO-0053	0.0095	0.0003	0.0082	0.0040	0.0059	0.0029
MO-0073	0.0150	0.0005	0.0201	0.0065	0.0145	0.0047
MO-0054	0.0190	0.0007	0.0274	0.0028	0.0197	0.0021
MO-0055	0.0235	0.0009	0.0279	0.0057	0.0201	0.0042
MO-0056	0.0275	0.0009	0.0402	0.0104	0.0291	0.0076
MO-0080	0.0330	0.0005	0.0450	0.0091	0.0325	0.0067
MO-0076	0.0410	0.0012	0.0600	0.0113	0.0436	0.0083
MO-0075	0.0480	0.0009	0.0734	0.0094	0.0536	0.0070
MO-0074	0.0510	0.0012	0.0817	0.0126	0.0598	0.0095
MO-0104	0.0550	0.0012	0.0724	0.0180	0.0529	0.0135

Table 4-1 The N concentration determined by HRXRD, x_{XRD}, and the N concentrations determined by Raman scattering, x_{Raman}, calculated using $f = 1$ and 1.4 of the GaAs$_{1-x}$N$_x$ alloy layers.

The result from Seong et al.'s measurements is displayed in Fig. 4-9. They have obtained the full circular data points using $f = 1.3$, giving the best linear fit for $x_{XRD} < 0.03$. However, a deviation from a linear dependence is observed for $x_{XRD} > 0.03$. Unlike Seong et al. [4], our result shows that x_{Raman} is linearly dependent on x_{XRD}. A linear dependence of Raman intensity of the N-related LVM mode on the N concentration provides a useful calibration method to determine the N concentration in dilute GaAs$_{1-x}$N$_x$ layers.
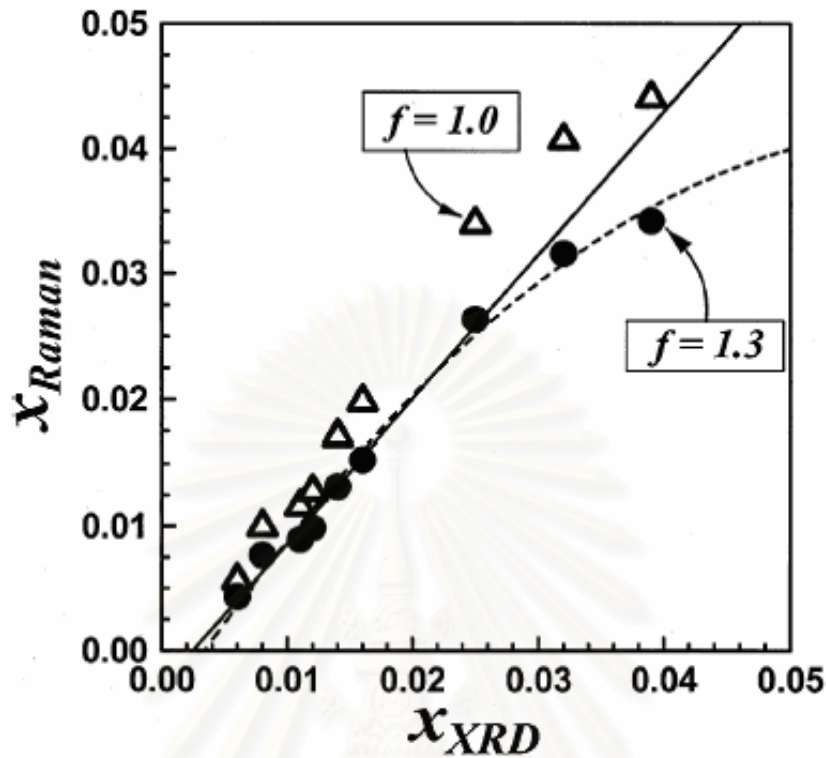
Fig. 4-9 The x_{Raman} as a function of the x_{XRD}, from Seong et al.'s experiment, where triangles are for f =1.0 and full circles are for f =1.3. The solid line represents a linear fit, $x_{Raman} = 1.145 x_{XRD} - 0.003$, to the data with f =1.3 for x_{XRD}<0.03 and the dashed line is an empirical quadratic fit $x_{Raman} = -12.2 x_{XRD}^2 + 1.51 x_{XRD} - 0.005$. Error bars are approximately the same as the diameter of full circle.

4.4 Summary

MOVPE grown GaAs$_{1-x}$N$_x$ strained layers on GaAs (001) substrates has been investigated by Raman scattering spectroscopy. It was found that, All the GaAs$_{1-x}$N$_x$ layers used in this study exhibit high alloy uniformity. The N concentration in the GaAs$_{1-x}$N$_x$ grown films determined by Raman spectroscopy technique, x_{Raman}, exhibits

a linear dependence on the x_{XRD}. The best fit using $f = 1.4$ yields $x_{\mathrm{Raman}} = x_{\mathrm{XRD}}$ for x_{XRD} ≤ 0.055. A linear dependence of x_{Raman} on x_{XRD}, provides a useful calibration method to determine the N concentration in dilute $\mathrm{GaAs_{1-x}N_x}$ alloys by using Raman spectroscopy technique.

CHAPTER V

NITROGEN DEPENDENCE OF BANDGAP ENERGY IN GaAsN ALLOY

5.1 Introduction

It is well known that bandgap energy of GaAs$_{1-x}$N$_x$ usually exhibit nonlinear bowing, and the change in the bandgap energy can be expressed as

$$E_{g,GaAsN} = x \cdot E_{g,GaN} + (1-x) \cdot E_{g,GaAs} + b \cdot x \cdot (1-x) \tag{5-1}$$

where b is bowing parameter. The bowing parameter is large and strongly depends on the N concentration with $b = 26$ eV for $x \leq 0.01$, $b = 16$ eV for $x > 0.01$ [31]. As presented in this equation, the change in the N concentration (x) leads to the strongly change in the bandgap energy of GaAs$_{1-x}$N$_x$ ($E_{g,GaAsN}$). Hence, the analysis of the bandgap energy of GaAs$_{1-x}$N$_x$ is vital, both for the clarification of fundamental controversy, and for the design of GaAs$_{1-x}$N$_x$ based devices. In this chapter, the change in bandgap energy of GaAs$_{1-x}$N$_x$ due to the incorporation of N into the lattice, was investigated. The experimental techniques used in this study are Fourier transform infrared (FTIR) spectroscopy and photoluminescence (PL).

FTIR spectroscopy is an analytical technique used to investigate the transition energy as well as the bandgap energy of materials. The infrared absorption bands identify specific molecular components and structures. Because the material absorbs infrared energy at specific frequency, the bandgap energy of the material can be determined by the spectral location of its infrared (IR) absorption.

PL is a powerful technique which typically using for investigation of the luminescence properties of materials. PL results on the $GaAs_{1-x}N_x$ films are sensitive tool for investigated the electronic states, impurity levels, and defects.

5.2 FTIR and PL Measurements

FTIR spectroscopy was done at The Gem and Jewelry Institute of Thailand, Faculty of Science, Chulalongkorn University. FTIR spectra were recorded at room temperature, and the spectral range was set at 0-14000 cm^{-1}. Photoluminescence were performed at Prof. Dr. Kentaro Onabe Laboratory, Department of Advanced Materials Science, The University of Tokyo. PL setup is shown in Fig. 5.1. The excitation energy was provided by Ar^+ power laser 514.5 nm (2.41 eV). The luminescent light from the sample is collected by the collecting lens then dispersed to the monochromator for distinguishing photon energy before count by the detector. The lock-in technology is applied to increase the signal-noise ratio. All PL spectra were recorded at 8.5 K.
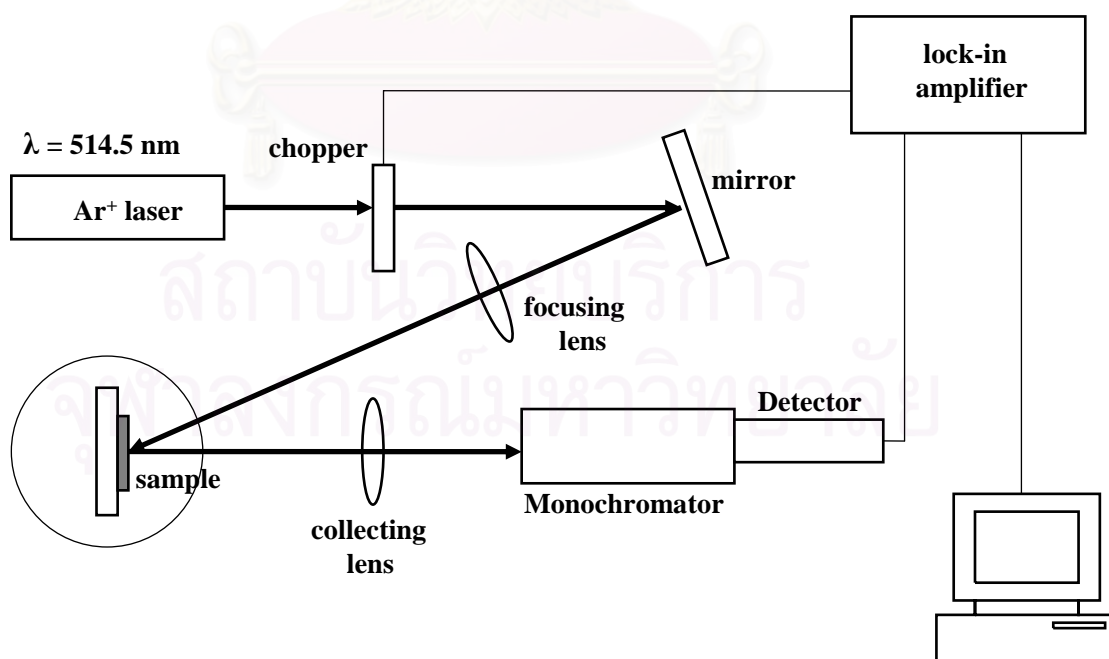
Fig. 5-1 Photoluminescence instrument set up.

5.3 Results and discussion

Figure 5-2 illustrates FTIR spectra of the GaAs$_{1-x}$N$_x$ films with different N concentrations. The bandgap energy of GaAs in wavenumber unit (11450 cm^{-1}) is given in this figure as red arrow. It is seen that the absorption bands of GaAs$_{1-x}$N$_x$ films have not changed with the N concentrations. All the GaAs$_{1-x}$N$_x$ samples, including GaAs sample absorb the same infrared energy. And, the absorption energy is lower than the bandgap energy of GaAs. Because of FTIR measurements not performed in vacuum, the absorption energy of air takes cover the absorption energy of GaAs and GaAs$_{1-x}$N$_x$. Thus, the results from FTIR spectroscopy can not be used to study the effect of N incorporation on the bandgap of the GaAs$_{1-x}$N$_x$ alloy films, due to the limit of the instrument.
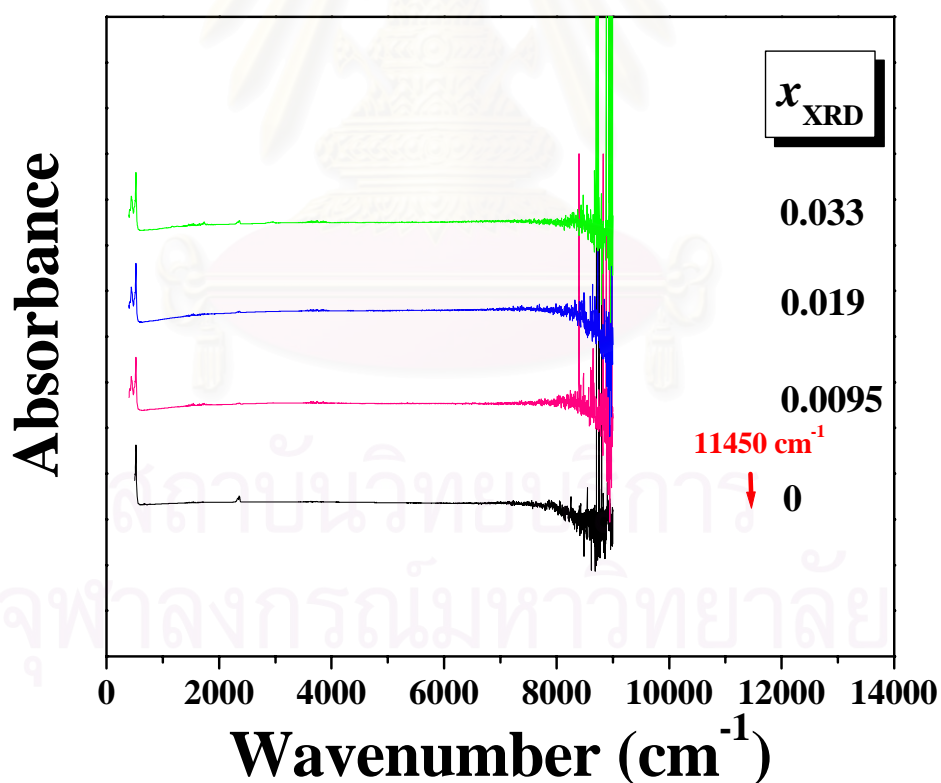
Fig. 5-2 The absorption bands of GaAs$_{1-x}$N$_x$ films with different N concentrations measured by Fourier transform infrared (FTIR) spectroscopy. The bangap energy of GaAs in wavenumber unit (11450 cm^{-1}) is indicated.

Photoluminescence (PL) is another technique which used to investigate the bandgap of two set of the GaAs$_{1-x}$N$_x$ samples. As-grown GaAs$_{1-x}$N$_x$ samples are the first set, and the second set is post growth thermal annealed GaAs$_{1-x}$N$_x$ samples. Figure 5-3 represents the low-temperature (8.5 K) PL spectra of both the as-grown (blue spectra) and the post growth thermal annealed (red spectra) GaAs$_{1-x}$N$_x$ samples. Values of the N concentrations and PL peak energy of each sample are also indicated, as shown in Fig. 5-3. The peak energy of PL spectra was varied from 1.39 to 0.97 eV with increasing the N concentrations from $x = 0.005$ to 0.0528.
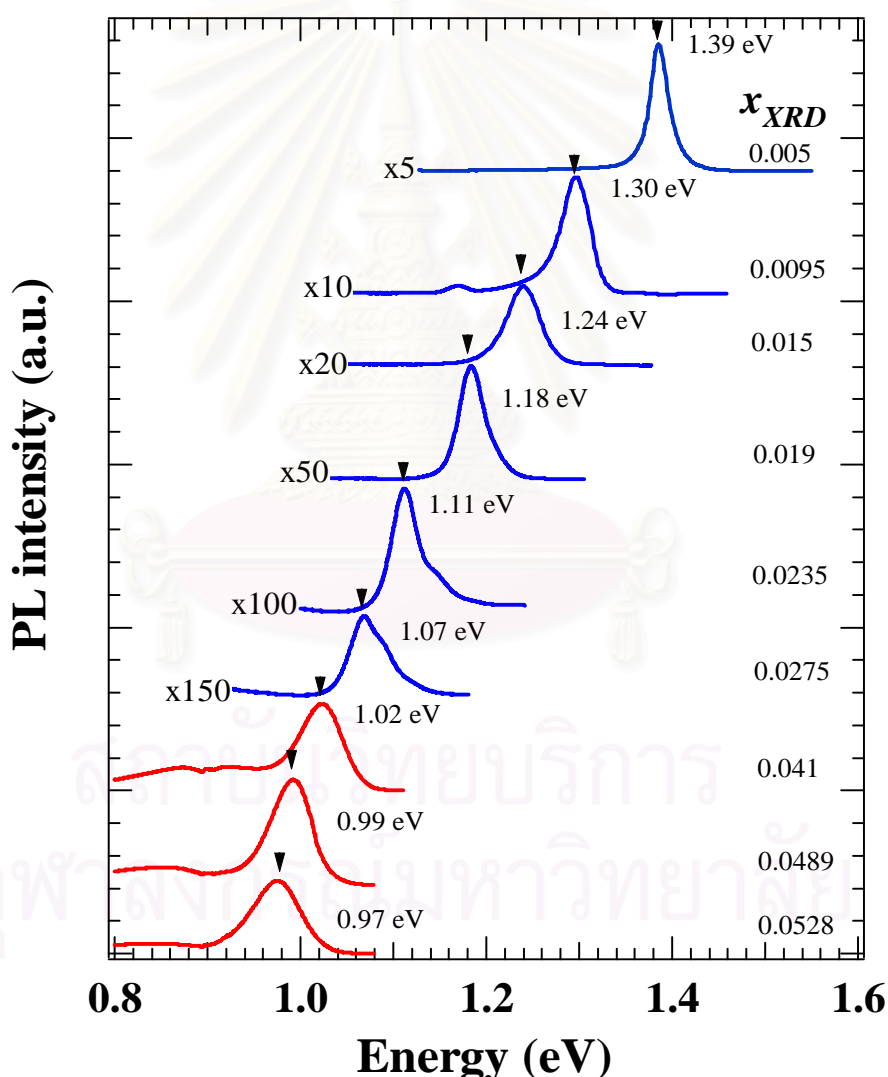
Fig. 5-3 The low-temperature (8.5 K) PL spectra of the GaAs$_{1-x}$N$_x$ alloy layers. The blue spectra and red spectra represent the PL spectra recorded from as-grown and annealed GaAs$_{1-x}$N$_x$ samples, respectively. The N concentration and PL peak energy are also indicated.

It is clearly observed that, the PL spectra have red shift when the N concentration is increased. The large red shift in PL spectra indicates a large bowing parameter (*b*) due to the N incorporation. These result similar to the result from other researches [11-13, 31]. The transition energy of $GaAs_{1-x}N_x$ as a function of the N concentration determined by Raman scattering (x_{Raman}) and the N concentration determined by high resolution X-ray diffraction (x_{XRD}) are shown in Fig. 5-4. As shown in this figure, it is clearly seen that the transition energy rapidly decrease with increasing the N concentration.
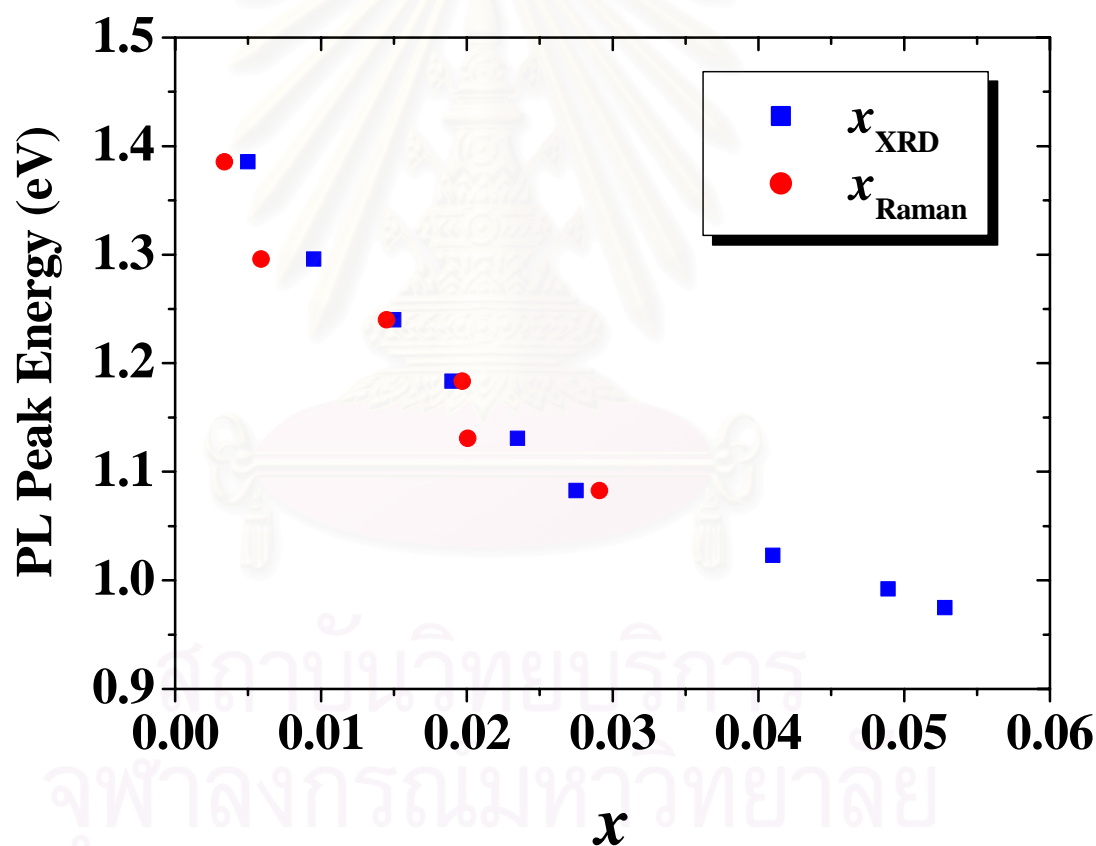
Fig. 5-4 The transition energy of $GaAs_{1-x}N_x$ as a function of the N concentration determined by Raman scattering (x_{Raman}) and the N concentration determined by high resolution X-ray diffraction (x_{XRD}). The blue square and red circle represented x_{XRD} and x_{Raman}, respectively.

Many research groups have used PL spectroscopy to study the bandgap energy of the GaAsN alloy. But, the results of different research groups scatter considerably, due to varying sample quality and inconsistencies in determining composition and bandgap energy. Some research groups showed that the transition energy is the bandgap energy [31-34], but the others presented the transition energy come from the N localized state near the bandgap of $GaAs_{1-x}N_x$ [35-43]. More experiments are required to clarify this point.
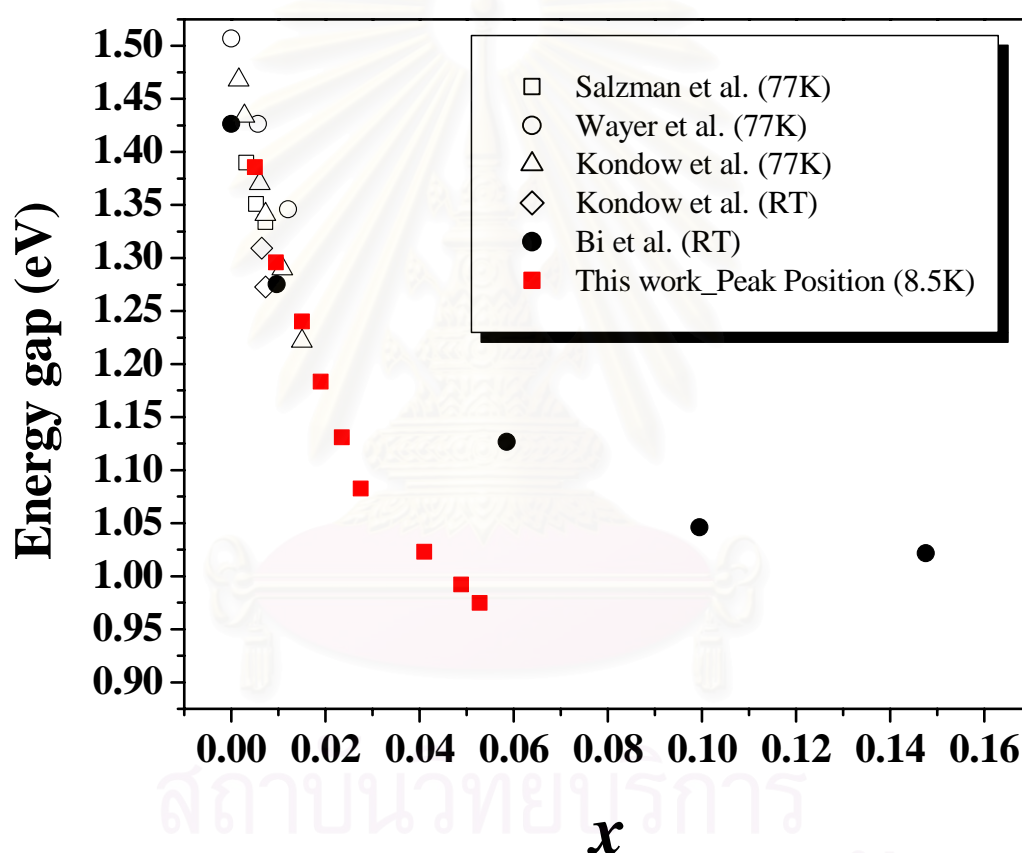
Fig. 5-5 The transition energy as a function of the N concentration, combined with the bandgap energy as a function of the N concentration measured in various laboratories [11].

Figure 5-5 shows the transition energy as a function of the N concentration, combined with bandgap energy as a function of the N concentration measured in various laboratories [11]. A large shrinkage of the bandgap energy for $x \leq 0.015$, and a

less shrinkage for higher values of x can be observed in this figure. The transition energy corresponding to the bandgap energy for the N concentration range of 0 - 0.015, and deviate from bandgap energy for greater values of the N concentrations. This is consistent with the suggestion that the transition energy indicated the bandgap energy for low N concentration. However, this conclusion has to be taken with caution, because the transition energy deviated from bandgap energy for greater values of the N concentrations.

5.4 Summary

The $GaAs_{1-x}N_x$ layers ($0 \leq x_{XRD} \leq 0.055$) have been investigated by Fourier transform infrared (FTIR) and photoluminescence (PL) spectroscopy. The absorption bands of $GaAs_{1-x}N_x$ alloy films measured by FTIR have not changed with the N concentrations. Thus, FTIR spectroscopy con not be used to study the effect of N incorporation on the bandgap of $GaAs_{1-x}N_x$ films, due to the limit of the instrument. A large red shift in low-temperature (8.5 K) photoluminescence spectra indicated a large bowing parameter due to the incorporation of N into the lattice. In addition, the transition energy observed by PL indicated the bandgap energy for a small amount of N concentrations ($x < 0.015$). On the other hand, the transition energy was deviated from the bandgap energy for the greater values of the N concentrations ($x > 0.015$).

CHAPTER VI

CONCLUSIONS

In this thesis, MOVPE grown $GaAs_{1-x}N_x$ ($0 \leq x_{XRD} \leq 0.055$) strained alloy layers on GaAs (001) substrates have been investigated. The goal of this thesis is to describe the compositional and optical properties of the $GaAs_{1-x}N_x$ thin films on GaAs, emphasize on the effect of N incorporation. High resolution X-ray diffraction (HRXRD), Raman scattering, Fourier transform infrared (FTIR), and Photoluminescence (PL) spectroscopes on $GaAs_{1-x}N_x$ films are described.

The structural quality and the N concentrations of $GaAs_{1-x}N_x$ alloy films have been investigated by HRXRD. It clearly observed that the $GaAs_{1-x}N_x$ alloy films which higher N contents up to 0.055, are still coherently strained and good epitaxial quality. The N concentrations in $GaAs_{1-x}N_x$ and the thickness of the $GaAs_{1-x}N_x$ films were determined by HRXRD measurement and simulation. The results from HRXRD measurement show a good agreement with the results from the simulation. This confirms that the N concentrations and the thickness of $GaAs_{1-x}N_x$ alloy layers obtained by HRXRD measurement are accurately determined.

Then, the $GaAs_{1-x}N_x$ layers have been studied by Raman scattering spectroscopy. It was found that, $GaAs_{1-x}N_x$ layers have high uniformity. And, in the N-incorporating films, a single N-related local vibrational mode (LVM) is observed at around 467 - 475 cm^{-1}. The normalized N-related LVM Raman intensity is proportional to the N concentration. The N concentration in the $GaAs_{1-x}N_x$ grown films determined by Raman spectroscopy technique (x_{Raman}), exhibits a linear dependence on the N concentration determined by HRXRD (x_{XRD}). The best fit using f = 1.4 yields $x_{Raman} = x_{XRD}$ for $x_{XRD} \leq 0.055$. A linear dependence of x_{Raman} on x_{XRD}, provides a useful calibration method to determine the N concentration in dilute $GaAs_{1-x}N_x$ alloys by using Raman spectroscopy technique.

FTIR and PL spectroscopes are used to investigate the bandgap of the

$GaAs_{1-x}N_x$ alloy. The absorption bands of $GaAs_{1-x}N_x$ measured by FTIR have not changed with the N concentrations. Thus, FTIR spectroscopy can not be used for study the effect of N incorporation on the bandgap of $GaAs_{1-x}N_x$ films, due to the limit of the instrument. A large red shift in low-temperature (8.5 K) PL spectra indicated a large bowing parameter in the $GaAs_{1-x}N_x$ alloy system due to the incorporation of N into the lattice.

Based on our results, the $GaAs_{1-x}N_x$ alloy shows unique electronic and physical properties which are useful for technological applications in optoelectronic devices. Hopefully, these results are useful for full understanding the compositional and optical properties of the $GaAs_{1-x}N_x$ alloy, and may be extended to explain the other III-V nitride alloys. Further work, it is necessary to clarify the effect of N incorporation on the physical parameters, especially bandgap energy.

REFERENCES

(1) Kondow, M., et al. GaInNAs: a novel material for long-wavelength semiconductor lasers. **IEEE, J. Select. Topics Quantum Electron** 3 (1997): 719.

(2) Kondow, M., et al. GaInNAs:A Novel Material for Long-Wavelength-Range Laser Diodes with Excellent High-Temperature Performnce. **Jpn. J. Appl. Phys.** 35 (1996): 1273.

(3) Kurtz, S. R., et al. InGaAsN solar cells with 1.0 eV band gap, lattice matched to GaAs. **Appl. Phys. Lett.** 74 (1999): 729.

(4) Seong, M. J.; Hanna, M. C.; and Mascarenhas, A. Composition dependence of Raman intensity of the nitrogen localized vibrational mode in $GaAs_{1-x}N_x$. **Appl. Phys. Lett.** 79 (2001): 3974-3976.

(5) Uesugi, K.; Morooka, N.; and Suemune, I. Reexamination of N composition dependence of coherently grown GaNAs band gap energy with high-resolution x-ray diffraction mapping measurements. **Appl. Phys. Lett.** 74 (1999): 1254-1256.

(6) Srnanek, R. et al. A Raman study of GaAsN,GaInAsN layers on beveled samples. **Mater. Sci. Eng. B** 91-92 (2002): 87-90.

(7) Toivonen, J. **Growth and properties of GaAsN structures**. Doctoral dissertation, Department of electrical and Communications Engineering, Helsinki University of Technology, 2003.

(8) Wayers, M.; Sato, M.; and Ando, H. Red shift of photoluminescence and absorption in dilute GaAsN alloy layers. **Jpn. J. Appl. Phys.** 31 (1992): L853.

(9) Hangleiter, A. III-V Nitrides: A New Age for Optoelectronics. **Mat. Res. Soc. Bulletin** (2003): 350-353.

(10) Sanorpim, S. **Structural and Optical Properties of III-III-V-N Type Alloy Films and Their Quantum wells**. Doctoral dissertation, Department of Applied Physics, Graduate School of Engineering, The University of Tokyo, 2003.

(11) Salzman, J.; and Temkin, H. III-V-N compounds for infrared applications. **Mater. Sci.Eng.** B50 (1997): 148-152.

(12) Buyanova, A.; Chen, W. M.; and Monemar, B. Electronic Properties of Ga(In)NAs Alloys. **Internet J. Nitride Semicond. Res. 6.** 2 (2001): 1-18.

(13) Kim, T. S., et al. Photocurrent measurements on $GaAs_{1-x}N_x$ epilayers grown by metalorganic chemical vapor deposition. **J. Crystal Growth** 260 (2004): 336-342.

(14) Vurgaftman, I.; Meyer, J. R.; and Ram-Mohan, L. R. Band parameters for III-V compound semiconductors and their alloys. **J. Appl. Phys.** 89 (2001): 5848-5849.

(15) Akasaki, I.; and Amano, H. Crystal growth and conductivity control of group III nitride semiconductors and their application to short wavelength light emitters. **Jpn. J. Appl. Phys.** 36 (1997): 5393.

(16) Sell, D. D.; Casey, H. C.; and Wecht, K. W. Concentration dependence of the refractive index for n- and p-type GaAs between 1.2 and 1.8 eV. **J. Appl. Phys**. 45 (1974): 2650.

(17) Bernard, G. **Group III Nitride Semiconductor compounds (Physics and Applications)**, 1998.

(18) Bateman, T. B.; McSkimin, H. J.; and Whelan, J. M. Elastic Moduli of Single-Crystal Gallium Arsenide. **J. Appl. Phys.** 30 (1959): 544.

(19) Mascarenhas, A.; and Seong, M. J. Raman and resonant Raman studies of $GaAs_{1-x}N_x$. **Semicond. Sci. Technol.** 17 (2002): 823-829.

(20) Kittel, C. **Introduction to Solid State Physics**. 7th ed. Canada: John Wiley & Sons, 1996.

(21) Yu, P. Y.; and Cardona, M. **Fundamentals of Semiconductors**. Berlin: Springer, 1996.

(22) Vijarnwannaluk, S. **Optical studies of GaAs:C grown at low temperature and of localized vibrations in normal GaAs:C**. Doctoral dissertation, Virginia Polytechnic Institute and State University, 2002.

(23) Alt, H. Ch.; Egorov, A. Y.; Riechert, H.; Meyer, J. D.; and Wiedemann, B. Incorporation of nitrogen in GaAsN and InGaAsN alloys investigated by FTIR and NRA. **Physica B** 308-310 (2001): 877-880.

(24) Nakajima, F.; Sanorpim, S.; Ono, W.; Katayama R.; and Onabe, K. MOVPE growth and optical characterization of GaAsN films with higher nitrogen concentrations. **Phys. Stat. Sol. A** 203 (2006): 1641-1644.

(25) Park, C. S., et al. The Influence of Well and Barrier Conditions on InGaAsN/GaAs Multiple Quantum Wells Grown by Using MOCVD. **J. Korean Phys. Soc.** 43 (2003): 1096-1099.

(26) Aspnes, D. E.; and Studna, A. A. Dielectric functions and optical parameters of Si, Ge, GaP, GaAs, GaSb, InP, InAs, and InSb from 1.5 to 6.0 eV. **Phys. Rev. B** 27 (1983): 985-1009.

(27) Mintairov, A. M., et al. Ordering effects in Raman spectra of coherently strained $GaAs_{1-x}N_x$. **Phys. Rev. B** 56 (1997): 15836-15841.

(28) Serries, D.; Geppert, T.; Kohler, K.; Ganser, P.; and Wagner, J. Dilute Group III-AsN: Bonding of Nitrogen in GaInAsN and AlGaAsN on GaAs and Realization of long Wavelength (2.3 μm) GaInAsN QWs on InP. **Mat. Res. Soc. Proc.** 744 (2003), M10.2.1.

(29) Alt, H. Ch. et al. Local vibrational mode absorption of nitrogen in GaAsN and InGaAsN layers grown by molecular beam epitaxy. **Physica B** 302-303 (2001): 282-290.

(30) Prokofyeva, T.; Sauncy, T.; Seon, M.; and Holtz, M. Raman studies of nitrogen incorporation in $GaAs_{1-x}N_x$. **Appl. Phys. Lett.** 73 (1998): 1409-1411.

(31) Tisch, U.; Finkman, E.; and Salzman, J. The anomalous bandgap bowing in GaAsN. **Appl. Phys. Lett.** 81 (2002): 463-465.

(32) Wang, L.; and Haegel, N. M. Optical Characterization of Heavily Carbon Doped GaAs. **Mat. Res. Soc. Proc.** 240 (1992): 87-91.

(33) Titkov, A. N.; Chaikina, E. I.; Komova, E. M.; and Ermakova, N. G.. Low-temperature luminescence of degenerate p-type crystals direct-gap semiconductors. **Sov. Phys. Semicond.** 15 (1981): 198-202.

(34) Wang, L.; and Haegel, N. M. Band-to-band photoluminescence and luminescence excitation in extremely heavily carbon-doped epitaxial GaAs. **Phys. Rev. B** 49 (1994): 10976-10985.

(35) Olego, D.; and Cardona, M. Photoluminescence in heavily doped GaAs. I. Temperature and hole-concentration dependence. **Phys. Rev. B** 22 (1980):

886-893.

(36) Bouzid, B. S.; Bousbih, F.; Chtourou, R.; and Tounie, E. Band gap energy, nitrogen localized states and GaN-like phonon in heavily doped GaAsN grown by molecular beam epitaxy. **Solid State Communications** 130 (2004): 121-124.

(37) Wang, S. Z.; Yoon, S. F.; Loke, W. K.; Liu, C. Y.; and Yuan, S. Origin of photoluminescence of GaAsN/GaN(001) layers grown by plasma-assisted solid source molecular beam epitaxy. **J. Crystal Growth** 255 (2003): 258-265.

(38) Gao, Q., et al. Metalorganic chemical vapor deposition of GaAsN epilayers:microstructures and optical properties. **J. Crystal Growth** 264 (2004): 92-97.

(39) Zhang, Y.; Mascarenhas, A.; and Geisz, J. F. Discrete and continuous spectrum of nitrogen-induced bound states in heavily doped GaAs$_{1-x}$N$_x$. **Phys. Rev. B** 63 (2001) : 085205.

(40) Zhang, Y.; and Mascarenhas, A. Isoelectronic impurity states in GaAs:N. **Phys. Rev. B** 61 (2000): 15562- 15564.

(41) Zhang, Y.; Mascarenhas, A.; Xin, H. P.; and Tu, C. W. Scaling of band-gap reduction in heavily nitrogen doped GaAs. **Phys. Rev. B** 63 (2001): 161303.

(42) Bouzid, B. S.; Bousbih, F.; Chtourou, R.; Harmand, J. C.; and Voisin, P. Effect of nitrogen in the electronic structure of GaAsN and GaInAs(N) compounds grown by molecular beam epitaxy. **Mater. Sci. Eng. B** 112 (2004): 64-68.

(43) Bousbih, F.; Bouzid, B. S.; Chtourou, R.; and Harmand, J. C. Exitons bound to nitrogen complexes in heavily doped GaAs$_{1-x}$N$_x$ grown on GaAs misoriented substrates. **Mater. Sci. Eng. B** 112 (2004): 50-53.

(44) Bousbih, F.; Bouzid, B. S.; Chtourou, R.; and Harmand, J. C. Observation of localization complexes and phonons replicas in heavily doped GaAs$_{1-x}$N$_x$. **Applied Surface Science** 226(2004): 41-44.

APPENDICES

ELSEVIER

Correlation between Raman intensity of the N-related local vibrational mode and N content in GaAsN strained layers grown by MOVPE

P. Panpech[a], S. Vijarnwannaluk[a], S. Sanorpim[a,*], W. Ono[b], F. Nakajima[b], R. Katayama[b], K. Onabe[b]

[a]*Department of Physics, Faculty of Science, SPRL, Chulalongkorn University, Phayathai Road, Pathumwan, Bangkok 10330, Thailand*
[b]*Department of Advanced Materials Science, The University of Tokyo, 5-1-5 Kashiwanoha, Kashiwa 277-8561, Japan*

Abstract

GaAs$_{1-x}$N$_x$ alloy films ($0 \leqslant x \leqslant 0.055$) grown on GaAs (0 0 1) substrates by metalorganic vapor phase epitaxy (MOVPE) using TBAs and DMHy as As and N precursors, respectively, have been investigated by Raman spectroscopy. It was found that, with incorporating N up to $x = 0.055$, a single N-related localized vibrational mode (LVM) is observed at around 468–475 cm^{-1}. We have investigated the N-related LVM Raman intensity (I_{LVM}) and frequency (ω_{LVM}) as a function of N concentration. Both the I_{LVM} and the ω_{LVM} were found to rise for the GaAs$_{1-x}$N$_x$ films with higher N incorporation. It is also evident that the N concentration in the GaAs$_{1-x}$N$_x$ grown films determined by Raman spectroscopy technique (x_{Raman}) exhibits a linear dependence on the N concentrations determined by the high resolution X-ray diffraction (HRXRD) (x_{XRD}). Our results demonstrate that the linear dependence of the x_{Raman} on the x_{XRD} provides a useful calibration method to determine the N concentration in dilute GaAs$_{1-x}$N$_x$ films ($x_{XRD} \leqslant 0.055$).
© 2006 Elsevier B.V. All rights reserved.

PACS: 78.30.−j; 63.20.−e; 63.20.Pw; 81.15.Kk

Keywords: A1. Compositional analysis; A1. High-resolution X-ray diffraction; A3. MOVPE; B1. GaAsN alloys; B1. III–V-nitrides; B2. Semiconducting ternary compounds

1. Introduction

GaAs$_{1-x}$N$_x$ and In$_y$Ga$_{1-y}$As$_{1-x}$N$_x$ have attracted interests because of their unique electronic and optical characteristics. It is well known that the incorporation of a small amount of N in GaAs$_{1-x}$N$_x$ leads to a decrease of the bandgap energy due to the large bandgap bowing, and to an increase of the electron effective mass. These alloys have been studied because of their potential applications in long-wavelength optoelectronic devices [1,2] and high-efficiency multijunction (MJ) solar cells [3]. A great deal of work has been done on the epitaxial growth and characterization of the III–V-N-type alloys in order to control the bandgap and electrical properties by controlling the alloy composition. While the bandgap and lattice constants as a function of the alloy composition for

GaAs$_{1-x}$N$_x$ have been studied [1–4], further work is obviously necessary to investigate the micro-(nano-)structural and optical properties of GaAs$_{1-x}$N$_x$ as a function of N concentration and determine the alloying effect of GaN on GaAs.

Raman spectroscopy is a powerful technique to obtain information on crystal structure through measuring the vibrations of the crystal lattice. Raman spectra provide a sensitive tool for studying the impurity incorporation in such structure and the structural defects [5]. It is known that N-related local vibrational mode (LVM) absorption is directly proportional to the N concentration in GaAs$_{1-x}$N$_x$. Seong et al. compared the N concentrations in GaAs$_{1-x}$N$_x$ determined by Raman spectroscopy technique (x_{Raman}) with those determined by X-ray diffraction (XRD) (x_{XRD}) [4]. They demonstrated that x_{Raman} exhibits a linear dependence on x_{XRD} for $x_{XRD} < 0.03$ and some deviation from the linear dependence for $x_{XRD} > 0.03$. In this paper, we first review the results of Raman

*Corresponding author. Tel.: +66 2 218 5110; fax: +66 2 253 1150.
E-mail address: sakuntam.s@chula.ac.th (S. Sanorpim).

spectroscopic studies on the local bonding of N in $GaAs_{1-x}N_x$ with N concentrations up to $x_{XRD} = 0.055$. Second, we describe the N concentration dependence of the LVM in $GaAs_{1-x}N_x$ films.

2. Experiments

2.1. Procedure

$GaAs_{1-x}N_x$ films were grown by low-pressure (60 Torr) MOVPE using trimethylgallium (TMG), dimethylhydrazine (DMHy) and tertiarybutylarsine (TBAs) as the source materials of Ga, N and As, respectively. Ultra-high purity H_2 was used as a carrier gas at flow rate of 1.5 slm. All GaAsN films were nominally un-doped and grown on semi-insulating (SI) GaAs (0 0 1) substrates at temperature ranging from 475 to 600 °C. An un-doped GaAs buffer layer of ~300 nm was first grown at 650 °C. The substrate temperature was then reduced to 450–600 °C for the growth of GaAsN layer (200–300 nm). The [TBAs]/ [TMGa] ratio was optimized to be 15. The flow rates of TMG and TBAs were fixed at 8.64 and 129.70 μmol/min, respectively. The flow rate of DMHy was varied in the range of 0–7000 μmol/min. N content in the GaAsN films was determined from a symmetrical (0 0 4) and an asymmetrical (1 1 5) high-resolution X-ray diffraction (HRXRD), assuming a linear dependence of lattice constant on the nitrogen concentration [6].

Micro-Raman scattering measurements were performed at room temperature (RT) using 514.5-nm-line Ar^+ laser as an excitation light source in backscattering geometry. The excitation laser beam was focused by a microscope lens system yielding a spot size ~2–4 μm in diameter.

3. Results and discussion

All $GaAs_{1-x}N_x$ films ($0 \leqslant x_{XRD} \leqslant 0.055$) in this study were examined by HRXRD in order to determine the N concentration and verify the structural quality. Fig. 1a shows a symmetric (0 0 4) HRXRD scans from a set of the $GaAs_{1-x}N_x$ films with different N contents. As shown in the figure, compared with GaAs, the peak shift to the higher diffraction angles was clearly observed with increasing N concentration, indicating the decrease of a lattice constant ($a_\perp$) normal to the (0 0 1) surface with the N incorporation. The narrow diffraction peaks and the clear Pendellösung fringes indicate that GaAsN films with high crystal quality were coherently grown on the GaAs substrate. An example of the reciprocal lattice mapping of an asymmetrical (1 1 5) reflection is shown in Fig. 1b for the $GaAs_{1-x}N_x$ film with N content of $x_{XRD} = 0.051$. This confirms that such high N-containing GaAsN layer is coherently strained and is of good epitaxial quality. These results are the evidence of high crystal quality films with higher N contents up to ~5%, obtained by the enhanced incorporation of N at lower growth temperatures (~500 °C) in spite of a large miscibility gap [7].
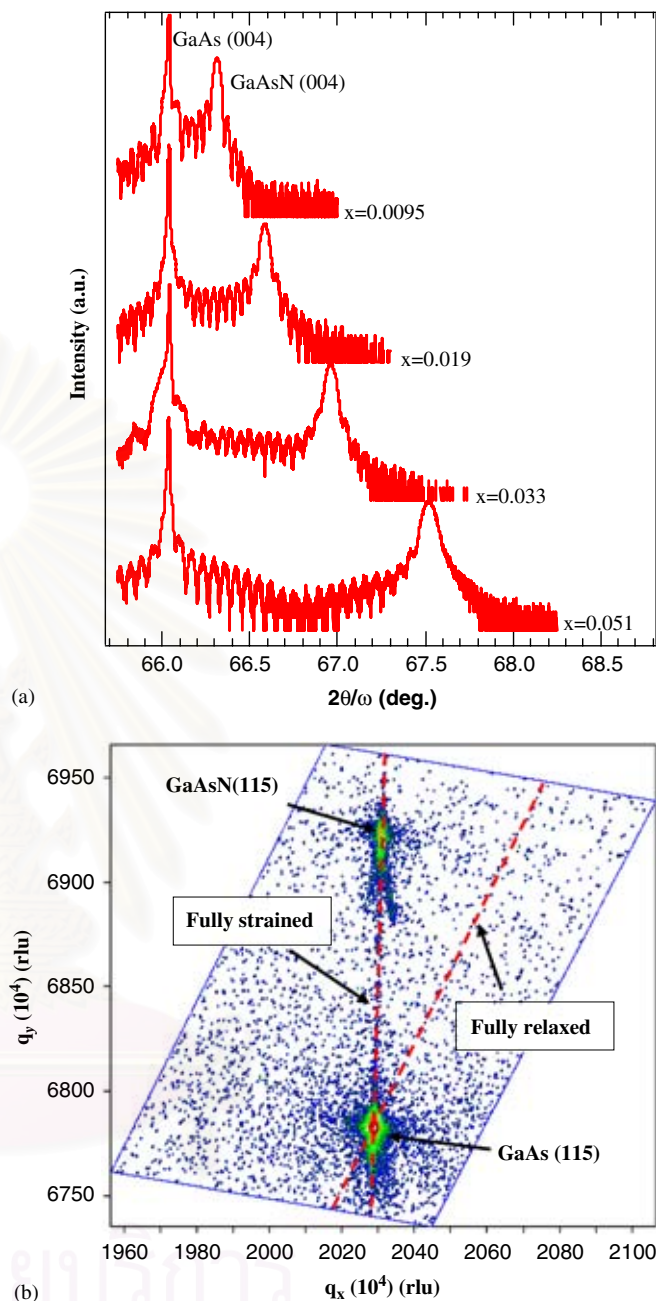

Fig. 1. (a) High-resolution (0 0 4) X-ray diffraction profiles of $GaAs_{1-x}N_x$ layers grown on the GaAs (0 0 1) substrates. Reciprocal lattice maps of the (1 1 5) reflection of the $GaAs_{1-x}N_x$ film with $x_{XRD} = 0.0051$ is shown in (b) as an example.

Fig. 2 shows typical Raman spectra recorded at room temperature (RT) for the $GaAs_{1-x}N_x$ film with N content of $x_{XRD} = 0.041$. Raman spectrum shows the transverse optical (TO) and longitudinal (LO) phonon modes of GaAs, along with a single N-related LVM. It is known that the Raman spectra taken from the GaAsN layer shows the GaN-like LO phonon mode, namely N-related LVM, at $470 \, cm^{-1}$ [8–10].

A sequence of room temperature Raman spectra taken from the $GaAs_{1-x}N_x$ films with N contents up to $x_{XRD} = 0.051$ is displayed in Fig. 3. The Raman intensity

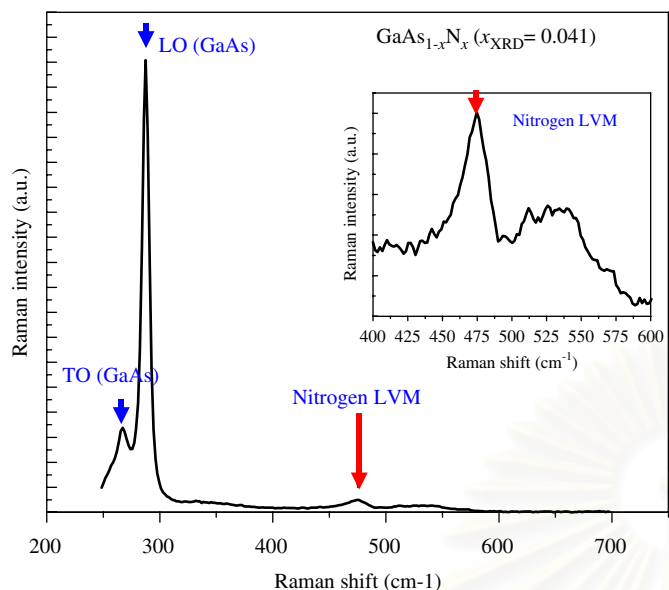Fig. 2. Raman spectra of GaAs$_{1-x}$N$_x$, for N content of $x_{XRD} = 0.041$, excited with Ar$^+$ 514.5 nm laser line at room temperature.
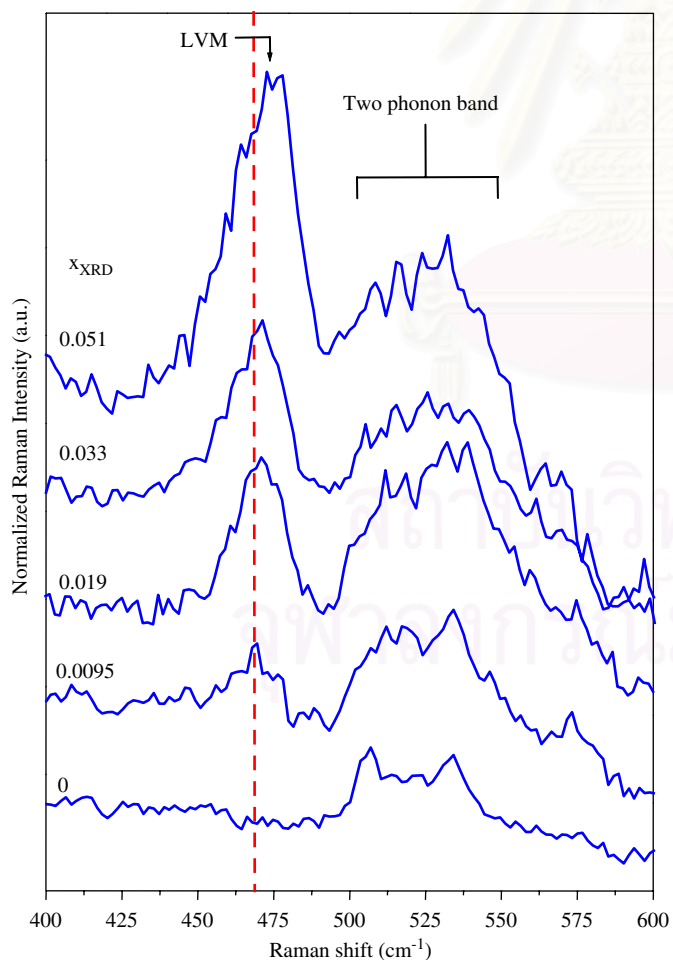
is normalized with respect to the GaAs-LO Raman intensity ($I_{GaAs-LO}$) for each sample and the base lines are subtracted. In the N-incorporating films, a single N-related LVM is observed at around 467–475 cm^{-1}. This mode has been attributed to the vibration associated with isolated N atoms each bonding to the four Ga neighbors [10]. It was observed that the normalized N-related LVM Raman intensity (I_{LVM}) was enhanced with increasing N concentration. As an expectation, the deterioration of the second-order Raman features of GaAs near 513 and 540 cm^{-1} [4] were clearly observed, shown in Fig. 3, due to the N incorporation. A gradual blue shift of the Raman frequency of the N-related LVM (ω_{LVM}) was also observed. In Fig. 4, the best fit yields $I_{LVM}/(I_{LVM} + I_{GaAs-LO}) = 1.43\,x_{XRD}$ and $\omega_{LVM} = 467.75 + 118.70\,x_{XRD}$.

It is known that the integrated intensity of GaAs-LO ($I_{GaAs-LO}$) in GaAs$_{1-x}$N$_x$ is proportional to As concentration and that of N-related LVM (I_{LVM}) is proportional to

Fig. 3. Raman spectra of GaAs$_{1-x}$N$_x$, for N concentrations of $x_{XRD} = 0$, 0.0095, 0.019, 0.033 and 0.051, excited with Ar$^+$ 514.5 nm laser line at room temperature.
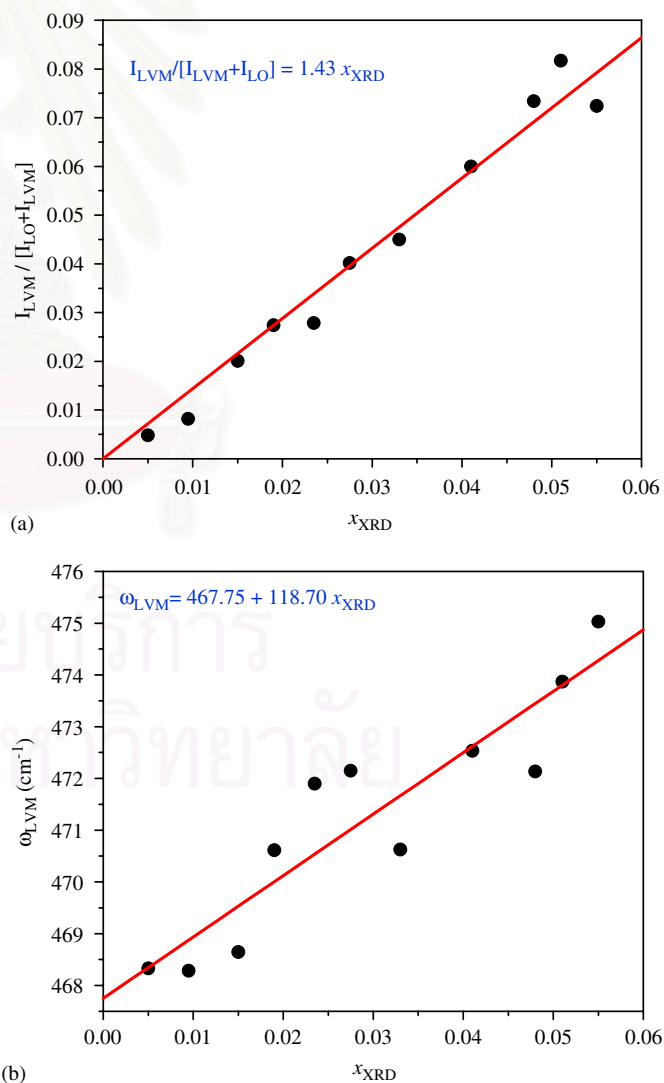

Fig. 4. The relationship of the $I_{LVM}/(I_{LVM} + I_{GaAs-LO})$ ratio, the Raman frequency of the N-related LVM (ω_{LVM}), and the N concentration (x_{XRD}) in the GaAs$_{1-x}$N$_x$ films.

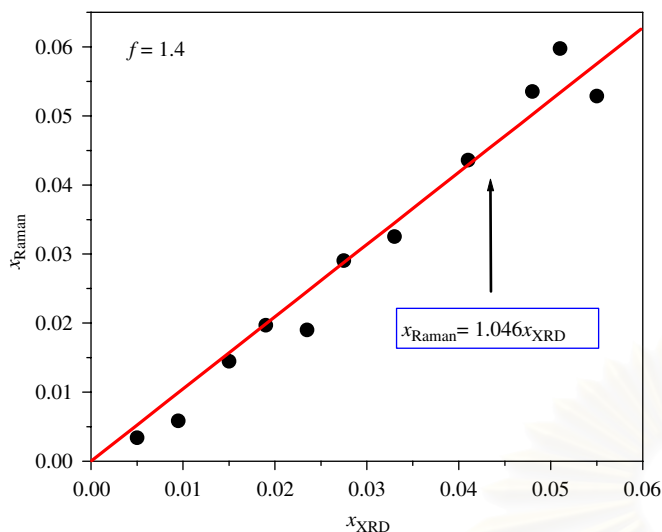*P. Panpech et al. / Journal of Crystal Growth 298 (2007) 107–110*

Fig. 5. The N concentrations, x_{Raman}, calculated using Eq. (1) as a function of N concentration determined by HRXRD measurement, x_{XRD}. The solid line represents a linear fit, $x_{\text{Raman}} = 1.046\, x_{\text{XRD}}$.

N concentration. Then x_{Raman} from the Raman measurement can be calculated as follows [4]:

$$x_{\text{Raman}} = \frac{I_{\text{LVM}}}{f I_{\text{GaAs-LO}} + I_{\text{LVM}}}, \qquad (1)$$

where f represents the relative N-related LVM oscillator strength with respect to that of the GaAs-LO phonon. The x_{Raman} calculated using the above equation as a function of x_{XRD} is displayed in Fig. 5. The data points were obtained using $f = 1.4$, giving the best fit ($x_{\text{Raman}} = 1.046\, x_{\text{XRD}}$) for the N contents up to $x_{\text{XRD}} = 0.055$. Unlike Seong et al. [4], our result shows that x_{Raman} is linearly dependent on x_{XRD}. A linear dependence of Raman intensity of the N-related LVM mode on the N concentration provides a useful calibration method to determine the N concentration in dilute $\text{GaAs}_{1-x}\text{N}_x$ layers.

4. Conclusions

Correlation between Raman intensity of the N-related LVM and N content in the MOVPE grown $\text{GaAs}_{1-x}\text{N}_x$ strained layers on GaAs (0 0 1) substrates were investigated. HRXRD results demonstrated that high crystal quality $\text{GaAs}_{1-x}\text{N}_x$ films with N contents up to $x_{\text{XRD}} = 0.055$ were successfully grown. The N concentration in the $\text{GaAs}_{1-x}\text{N}_x$ grown films determined by Raman spectroscopy technique, x_{Raman}, exhibits a linear dependence on the x_{XRD}. The best fit using $f = 1.4$ yields $x_{\text{Raman}} = 1.046\, x_{\text{XRD}}$ for $x_{\text{XRD}} \leqslant 0.055$. A linear dependence of x_{Raman} on x_{XRD}, provides a useful calibration method to determine the N concentration in dilute $\text{GaAs}_{1-x}\text{N}_x$ alloys by using Raman spectroscopy technique.

References

[1] M. Kondow, T. Kitatani, S. Nakatsuka, M.C. Larson, K. Nakahara, Y. Yazawa, M. Okai, IEEE J. Select. Topics Quantum Electron 3 (1997) 719.
[2] M. Kondow, K. Uomi, A. Niwa, T. Kitatani, S. Watahiki, Y. Yazawa, Jpn. J. Appl. Phys. 35 (1996) 1273.
[3] S.R. Kurtz, A.A. Allerman, E.D. Jones, J.M. Gee, J.J. Banas, B.E. Hammons, Appl. Phys. Lett. 74 (1999) 729.
[4] M.J. Seong, M.C. Hanna, A. Mascarenhas, Appl. Phys. Lett. 79 (2001) 3974.
[5] R. Srnanek, A. Vincze, J. Kovac, I. Gregora, D.S. Mc Phail, V. Gottschalch, Mater. Sci. Eng. B 91 (2002) 87.
[6] K. Uesugi, N. Morooka, I. Suemune, Appl. Phys. Lett. 74 (9) (1999) 1254.
[7] F. Nakajima, S. Sanorpim, W. Ono, R. Katayama, K. Onabe, Phys. Stat. Sol. a 203(2006) 1641.
[8] A.M. Mintairov, P.A. Blagnov, V.G. Melehin, N.N. Faleev, J.L. Merz, Y. Qiu, S.A. Nikishin, H. Temkin, Phys. Rev. B 56 (24) (1997) 15836.
[9] D. Serries, T. Geppert, K. Kohler, P. Ganser, J. Wagner, Mat. Res. Soc. Proc. 744 (2003) M10.2.1.
[10] H.ch. Alt, A.Yu. Egorov, H. Riechert, B. Wiedemann, J.D. Meyer, R.W. Michelmann, K. Bethge, Physica B 302–303 (2001) 282.

VITAE

Miss Panatda Panpech was born on June 18, 1982 in Suphanburi, Thailand. She received her bachelor degree of Science in Physics from Silpakorn University in 2004, and continued her Master's study at Chulalongkorn University in 2004.

Publications and Conference Presentations:

[1] **P. Panpech**, S. Vijarnwannaluk, S. Sanorpim, W. Ono, F. Nakajima, R. Katayama and K. Onabe, **"Correlation between Raman intensity of the N-related local vibrational mode and N content in GaAsN strained layers grown by MOVPE"** Journal of Crystal Growth 298 (2007): 107-110.

1 **P. Panpech**, S. Vijarnwannaluk, S. Sanorpim, W. Ono, F. Nakajima, R.Katayama and K. Onabe, **"Raman scattering study on the N-related local vibrational mode in GaAsN films"** Faculty of Science, Chulalongkorn University, 16-17 March, (2006).

2 **P. Panpech**, S. Vijarnwannaluk, S. Sanorpim, W. Ono, F. Nakajima, R. Katayama and K. Onabe, **"Determination of nitrogen concentration in GaAsN film by Raman scattering"** 32rd Congress on Science and Technology of Thailand, Queen Sirikit National Convention Center, 10-12 October, (2006).

3 **P. Panpech**, S. Vijarnwannaluk, S. Sanorpim, W. Ono, F. Nakajima, R. Katayama and K. Onabe, **"Investigation of nitrogen composition in GaAsN films by Raman scattering"** 6th Grad Research, Chulalongkorn University, 13-14 October, (2006).

4 **P. Panpech**, S. Vijarnwannaluk, S. Sanorpim, F. Nakajima, R. Katayama and K. Onabe, **"Optical Investigation of GaAs$_{1-x}$N$_x$ Alloy Films"** SPC 2007, Nakorn pathom, 22-24 March, (2007).